SAND2022-7077C

Physics Department
College of Science
University of Nevada, Reno

Photon Doppler velocimetry diagnosis of plasma electron density

K. J. Swanson, G. S. Jaar, R. C. Mancini, D. C. Mayes, V. V. Ivanov, A. L. Astanovitskiy, O. Dmitriev, A. W. Klemmer

Physics Department, University of Nevada, Reno, Nevada 89557, USA

C. De La Cruz, D. Dolan, A. Porwitzky, G. P. Loisel, J. E. Bailey, K. Bell

Sandia National Laboratories, Albuquerque, New Mexico 87185, USA

High-Temperature Plasma Diagnostics Conference · Rochester, NY · May 15 – 19, 2022

A new interferometric diagnostic successfully revealed electron-density time histories of laboratory photoionized plasma for the first time

- Time and spatially resolved measurements of electron density are a critical plasma diagnostic
- Photon Doppler velocimetry has been successfully implemented in close proximity to the x-ray flux produced by Z
- Dual PDV probes were used to assess plasma uniformity

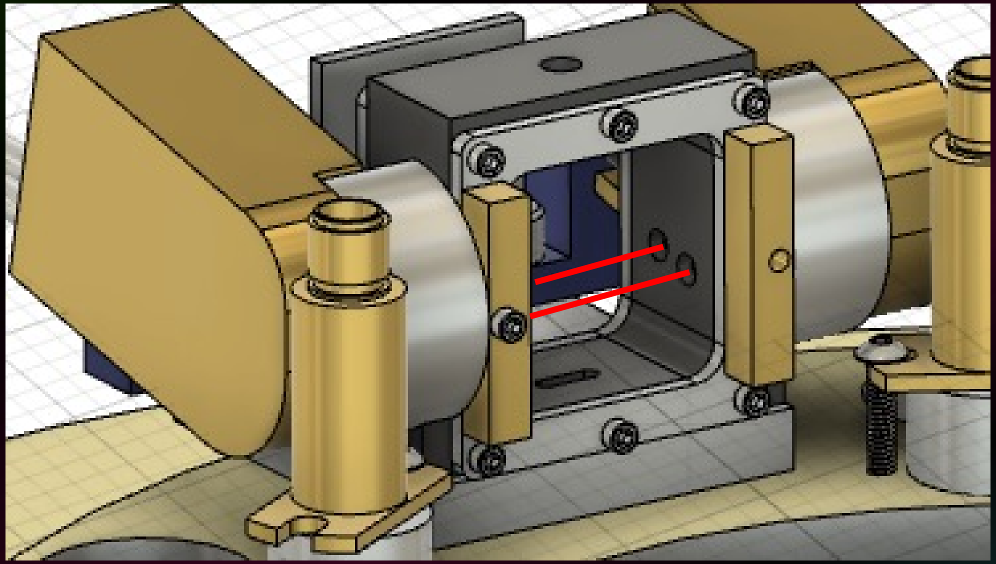

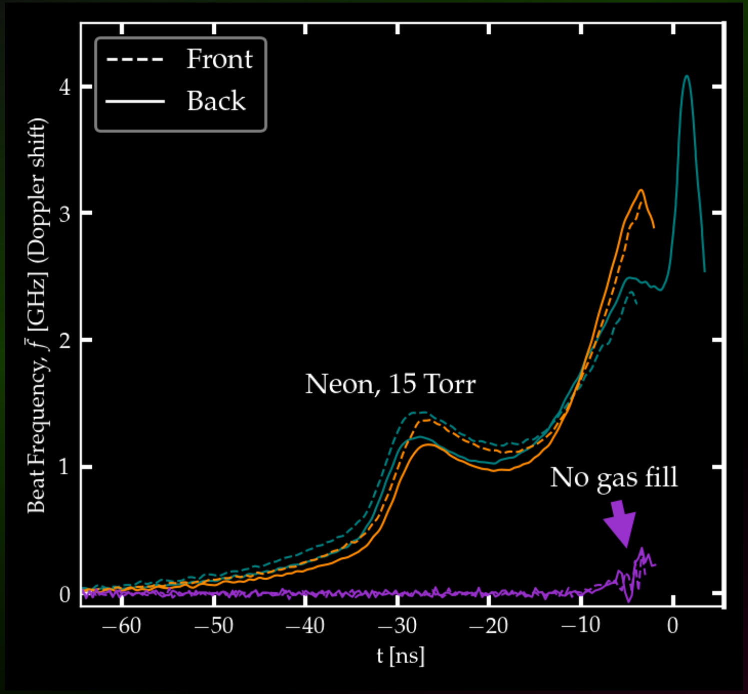

- We can refine our understanding of the experiment by combining laser and x-ray diagnostics
- We can test the accuracy of simulated electron density time history

We are using the Z-machine to investigate laboratory produced photoionized plasmas

- Photoionized plasmas are ubiquitous throughout space.
  - Ex: Active galactic nuclei, x-ray binary systems, and planetary nebulae

- Untested astrophysical models require high quality lab data[1,2]
  - Observations from orbiting telescopes Chandra and XMM Newton
  - Analyzed with codes, e.g. Cloudy & XStar, developed mainly on a best-theory effort

- Laboratory produced photoionized plasmas relevant to astrophysics require high intensity broadband x-ray flux.

- This requirement has usually relegated laboratory photoionized plasma work to large scale facilities developed for inertial confinement fusion experiments[3-7]

- The photoionized gas cell platform on the Z-machine allows investigation of laboratory produced photoionized plasmas

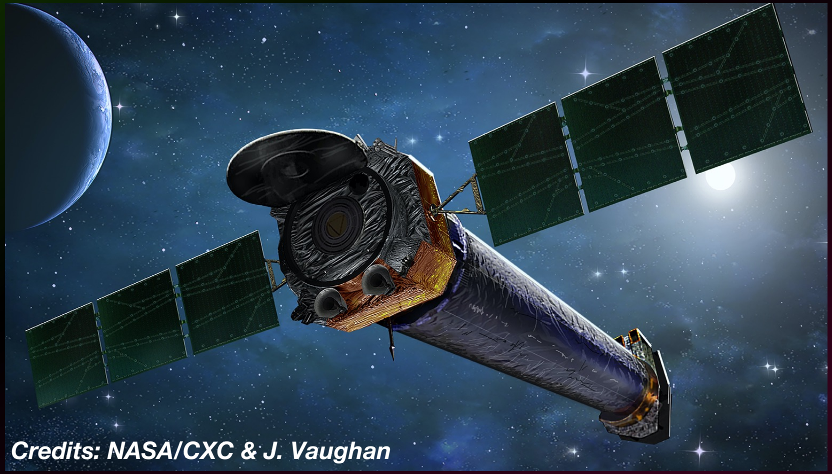
Credits: NASA/CXC & J. Vaughan


Credit: NASA/ESA/STScI

1) R. C. Mancini et al Phys. Plasmas **16**, 041001 (2009) 2**)** R. C. Mancini et al Phys. Rev. E 101, 051201 (2020) 3**)** M. E. Foord Phys. Rev. Letters **93**, 055002 (2004);
4**)** S. Fujioka et al Nature Physics **5**, 821 (2009); **5)** F. Wang et al, Phys. Plasmas **15**, 073108 (2008); 6**)** I. M. Hall et al, Phys. Plasmas **21**, 031203 (2014);
7**)** G. P. Loisel et al Phys. Rev. Letters **119**, 075001 (2017)

Gas cell platform on Z

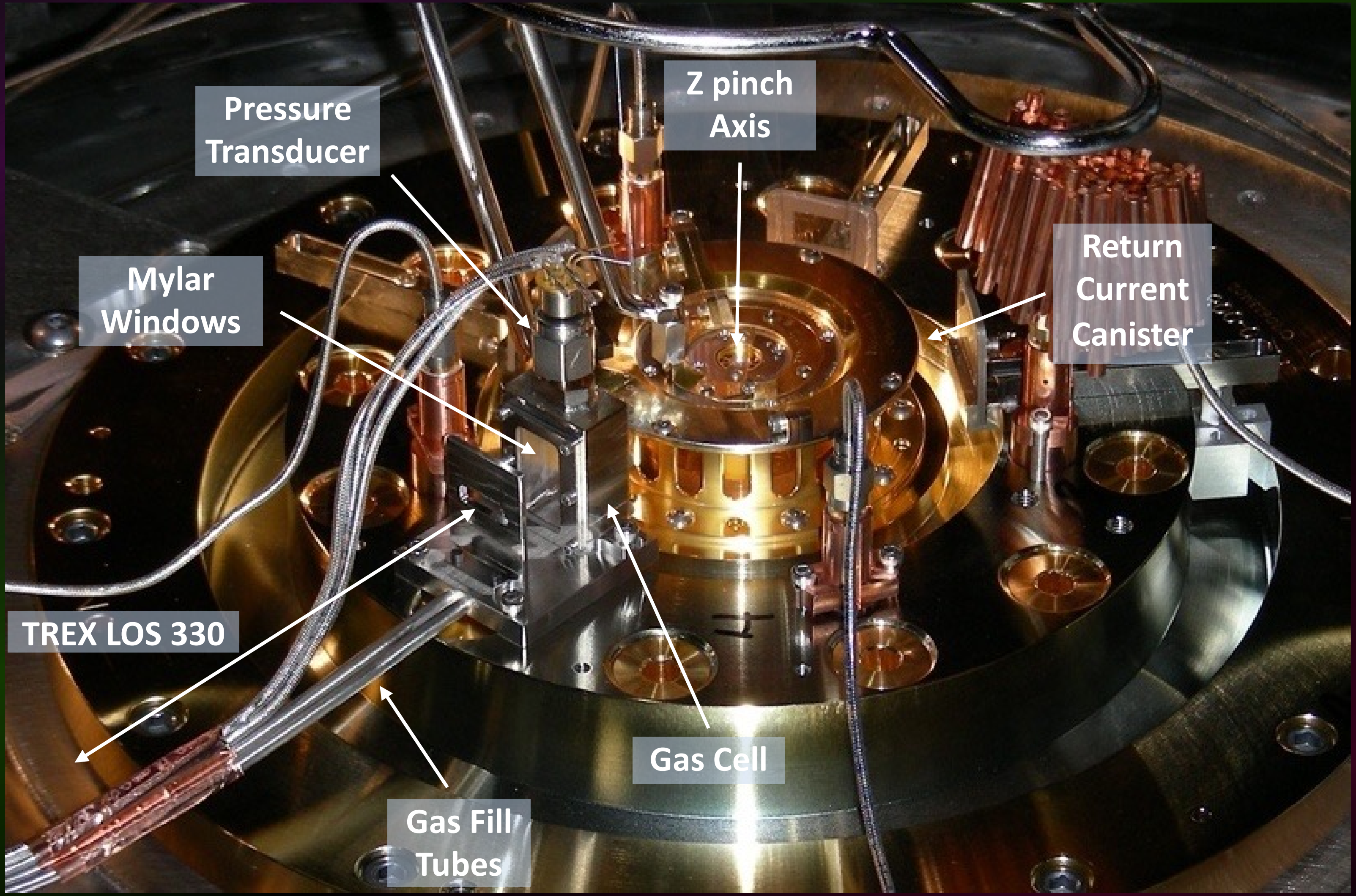

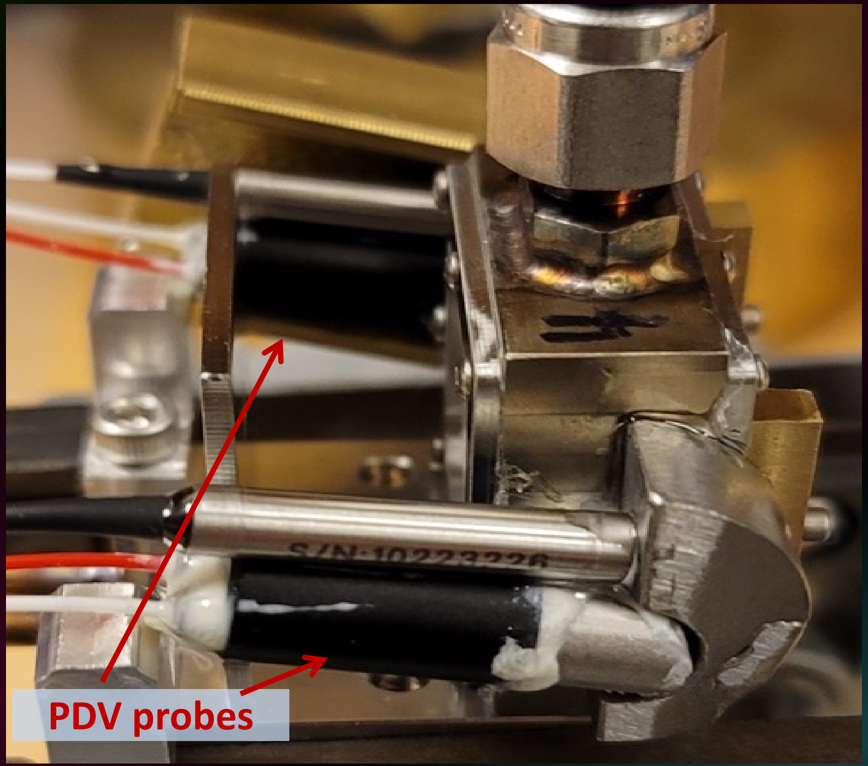

1. I. M. Hall et al. Phys. Plasmas 21, 031203, (2014)
2. K. J. Swanson et al. RSI, 93.4, 043502, (2022)

We can control ionization parameters by adjusting gas cell position and fill pressure

Ionization Parameter[1,2]

$$\xi = \frac{4\pi F}{n_e} \quad \left[\frac{erg \cdot cm}{s}\right]$$

A measure of the relative importance of photoionization and collisional ionization

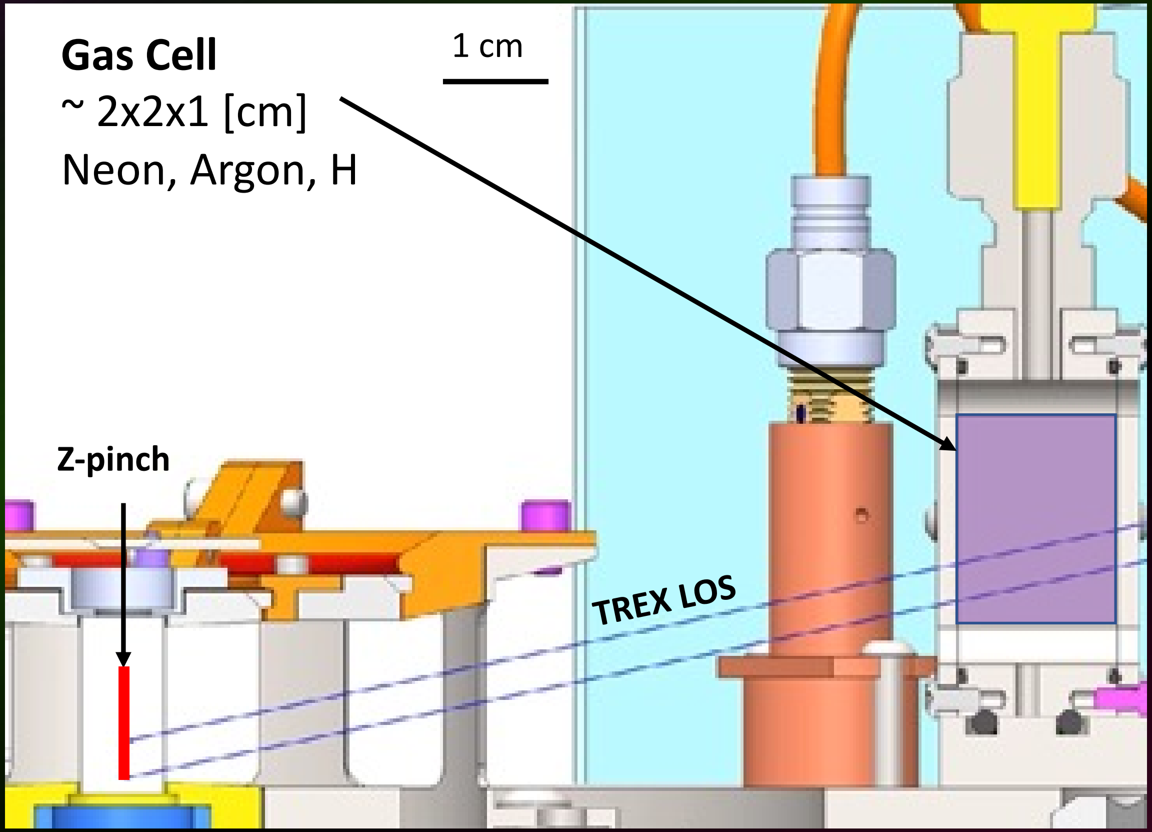

1) C. B. Tarter, et al. *ApJ*. 156, 943, (1969) 2) J.E. Bailey, et al. *JQSRT*. 71, 157, (2001) 3) R. C. Mancini, et al. PRE 101, 051201, (2020)
2) 4) D. C. Mayes, et al. PRE 104, 035202 (2021) 5) P. Lake, et al. RSI, 77, 10F315, (2006)

We can control ionization parameters by adjusting gas cell position and fill pressure

Ionization Parameter[1,2]

$$\xi = \frac{4\pi F}{n_e} \quad \left[\frac{erg \cdot cm}{s}\right]$$

A measure of the relative importance of photoionization and collisional ionization

Astrophysically relevant

$$\xi \gg 1$$

Achievable Ionization Parameters[3, 4]

$$\xi \approx 5 - 60$$

Two "knobs"

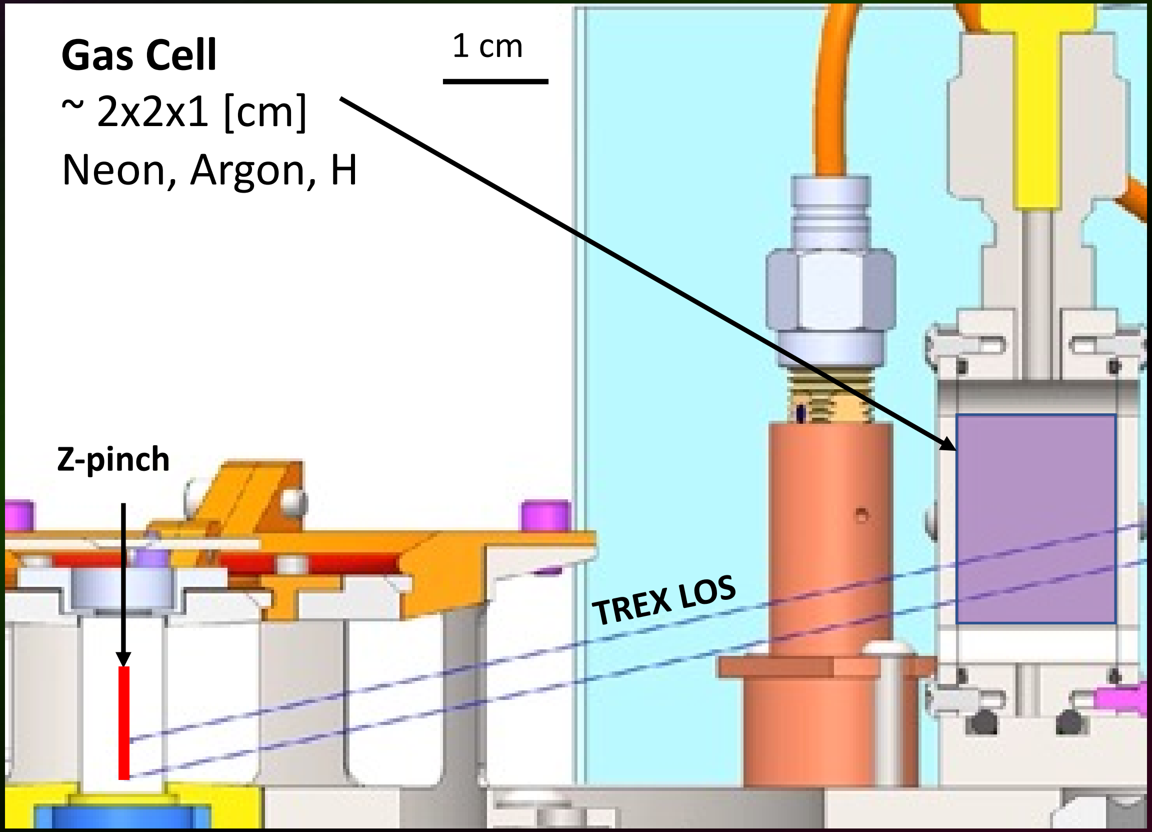

1) C. B. Tarter, et al. *ApJ*. 156, 943, (1969) 2) J.E. Bailey, et al. *JQSRT*. 71, 157, (2001) 3) R. C. Mancini, et al. PRE 101, 051201, (2020)
2) 4) D. C. Mayes, et al. PRE 104, 035202 (2021) 5) P. Lake, et al. RSI, 77, 10F315, (2006)

We can control ionization parameters by adjusting gas cell position and fill pressure

Ionization Parameter[1,2]

$$\xi = \frac{4\pi F}{n_e} \quad \left[\frac{erg \cdot cm}{s}\right]$$

A measure of the relative importance of photoionization and collisional ionization

Astrophysically relevant

$$\xi \gg 1$$

Achievable Ionization Parameters[3, 4]

$$\xi \approx 5 - 60$$

Two "knobs" → Density, →

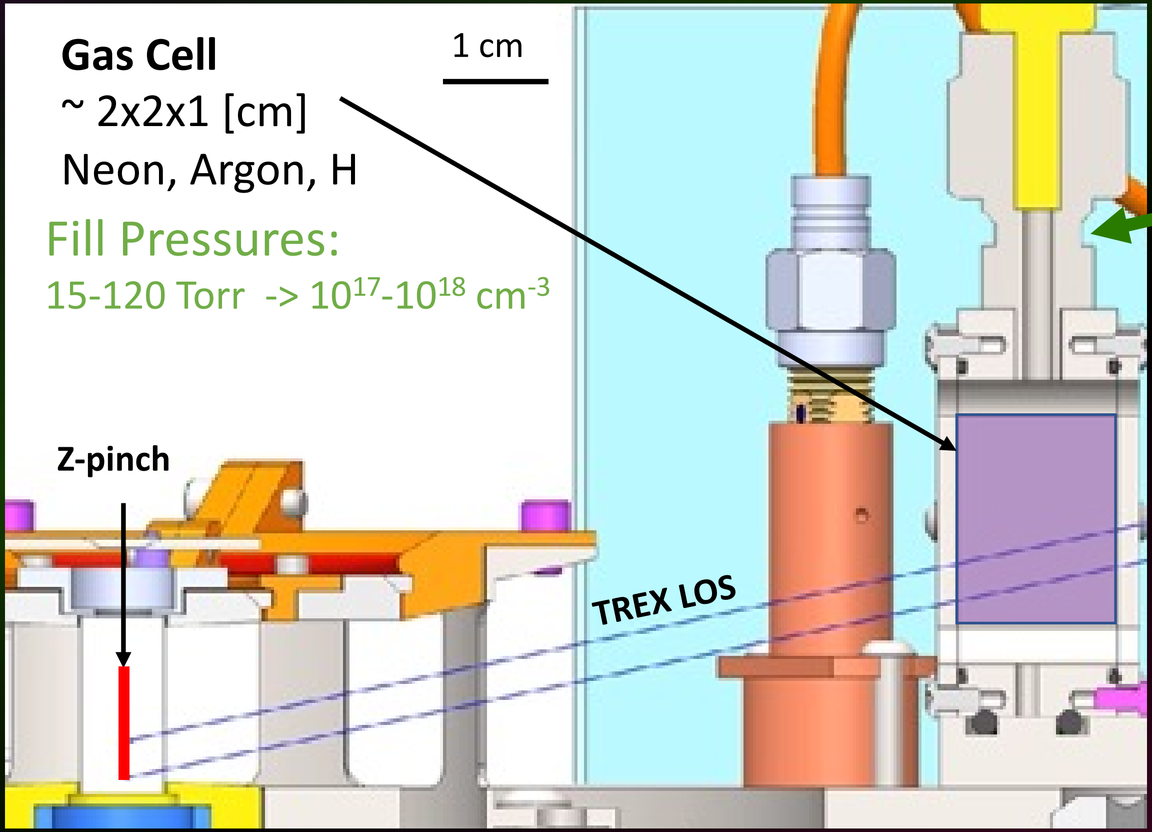

Pressure sensor

Density up to shot time

1) C. B. Tarter, et al. *ApJ*. 156, 943, (1969) 2) J.E. Bailey, et al. *JQSRT*. 71, 157, (2001) 3) R. C. Mancini, et al. PRE 101, 051201, (2020)
2) 4) D. C. Mayes, et al. PRE 104, 035202 (2021) 5) P. Lake, et al. RSI, 77, 10F315, (2006)

We can control ionization parameters by adjusting gas cell position and fill pressure

Ionization Parameter[1,2]

$$\xi = \frac{4\pi F}{n_e} \quad \left[\frac{erg \cdot cm}{s}\right]$$

A measure of the relative importance of photoionization and collisional ionization

Astrophysically relevant

$$\xi \gg 1$$

Achievable Ionization Parameters[3, 4]

$$\xi \approx 5 - 60$$

Two "knobs"
- Density
- Flux

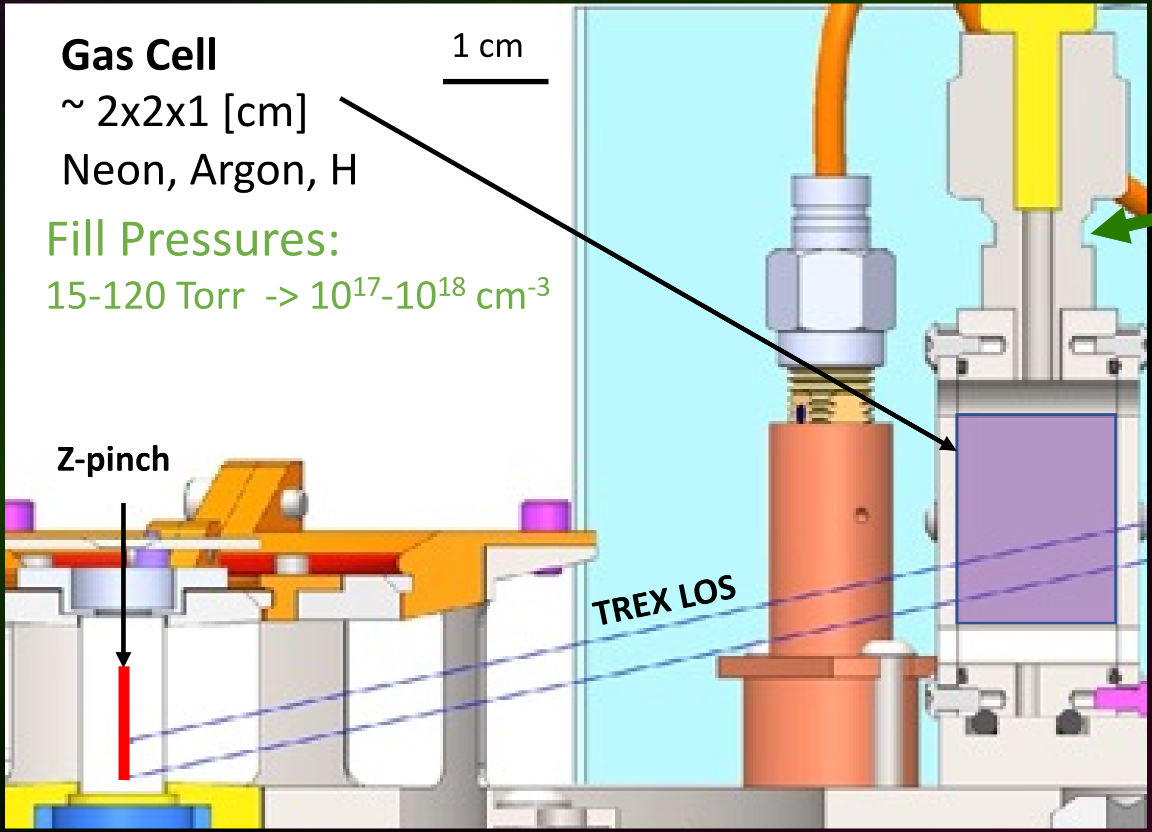

Pressure sensor
Density up to shot time

Gas cell positions:

Close Position: 4.3 cm => ~1.3x10^{12} W/ cm^2

Far Position: 5.9 cm => ~0.6x10^{12} W/ cm^2

1) C. B. Tarter, et al. *ApJ*. 156, 943, (1969) 2) J.E. Bailey, et al. *JQSRT*. 71, 157, (2001) 3) R. C. Mancini, et al. PRE 101, 051201, (2020)
2) 4) D. C. Mayes, et al. PRE 104, 035202 (2021) 5) P. Lake, et al. RSI, 77, 10F315, (2006)

We can control ionization parameters by adjusting gas cell position and fill pressure

Ionization Parameter[1,2]

$$\xi = \frac{4\pi F}{n_e} \quad \left[\frac{erg \cdot cm}{s}\right]$$

A measure of the relative importance of photoionization and collisional ionization

Astrophysically relevant

$$\xi \gg 1$$

Achievable Ionization Parameters[3, 4]

$$\xi \approx 5 - 60$$

Two "knobs"
- Density
- Flux

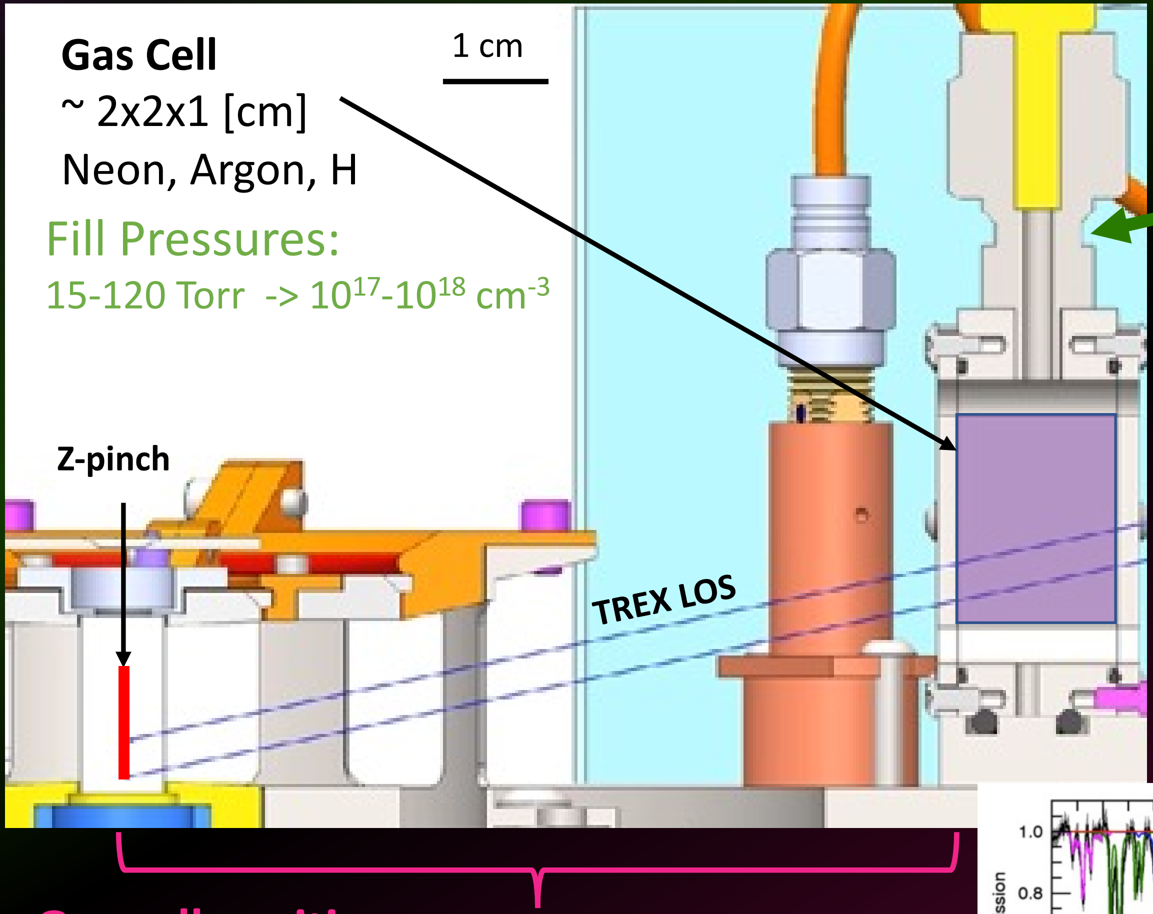

Gas cell positions:

Close Position: 4.3 cm => ~1.3x10^{12} W/ cm^2

Far Position: 5.9 cm => ~0.6x10^{12} W/ cm^2

Pressure sensor

Density up to shot time

TREX Spectrometer[4]

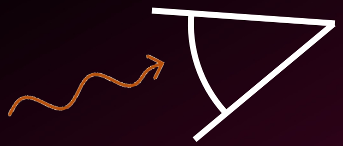

- Observes neon K-shell absorption spectra
- Photon energy range: 860-1230 eV
- Extract charge state distribution and electron temperature

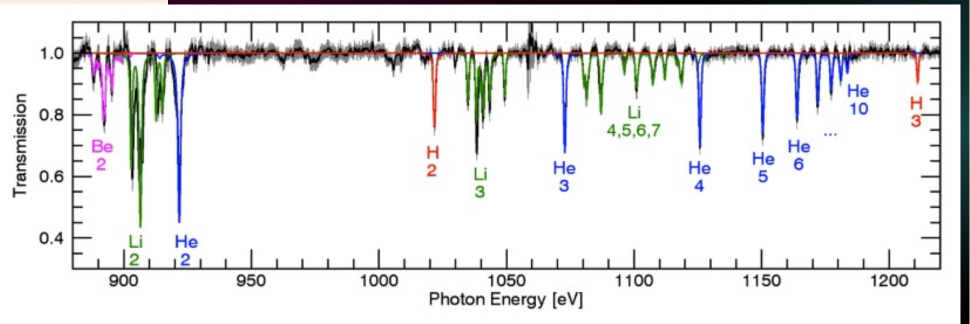

1) C. B. Tarter, et al. *ApJ*. 156, 943, (1969) 2) J.E. Bailey, et al. *JQSRT*. 71, 157, (2001) 3) R. C. Mancini, et al. PRE 101, 051201, (2020)
2) 4) D. C. Mayes, et al. PRE 104, 035202 (2021) 5) P. Lake, et al. RSI, 77, 10F315, (2006)

We can control ionization parameters by adjusting gas cell position and fill pressure

Ionization Parameter[1,2]

$$\xi = \frac{4\pi F}{n_e} \quad \left[\frac{erg \cdot cm}{s}\right]$$

A measure of the relative importance of photoionization and collisional ionization

Astrophysically relevant

$$\xi \gg 1$$

Achievable Ionization Parameters[3, 4]

$$\xi \approx 5 - 60$$

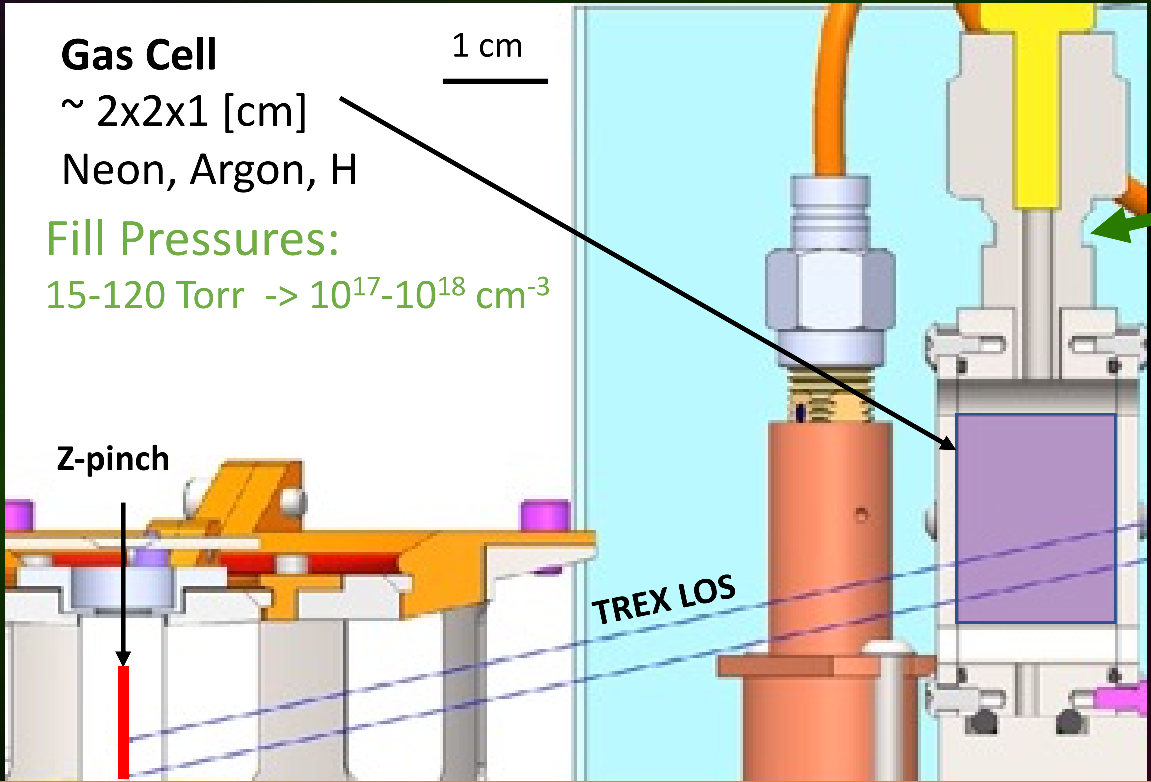

Pressure sensor

Density up to shot time

TREX Spectrometer[4]

- Observes neon K-shell absorption spectra
- Photon energy range: 860-1230 eV
- Extract charge state distribution and electron temperature

Two “knobs”

Flux

Important, to be able to diagnose conditions inside gas cell

Close Position: 4.3 cm => ~1.3x10^{12} W/ cm^2

Far Position: 5.9 cm => ~0.6x10^{12} W/ cm^2

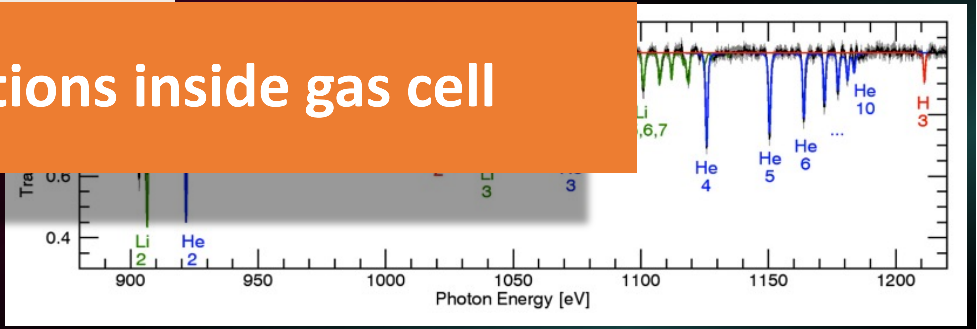

1) C. B. Tarter, et al. *ApJ*. 156, 943, (1969) 2) J.E. Bailey, et al. *JQSRT*. 71, 157, (2001) 3) R. C. Mancini, et al. PRE 101, 051201, (2020)
2) 4) D. C. Mayes, et al. PRE 104, 035202 (2021) 5) P. Lake, et al. RSI, 77, 10F315, (2006)

Simulations predict a central region of quasi hydro-unperturbed photoionized neon plasma

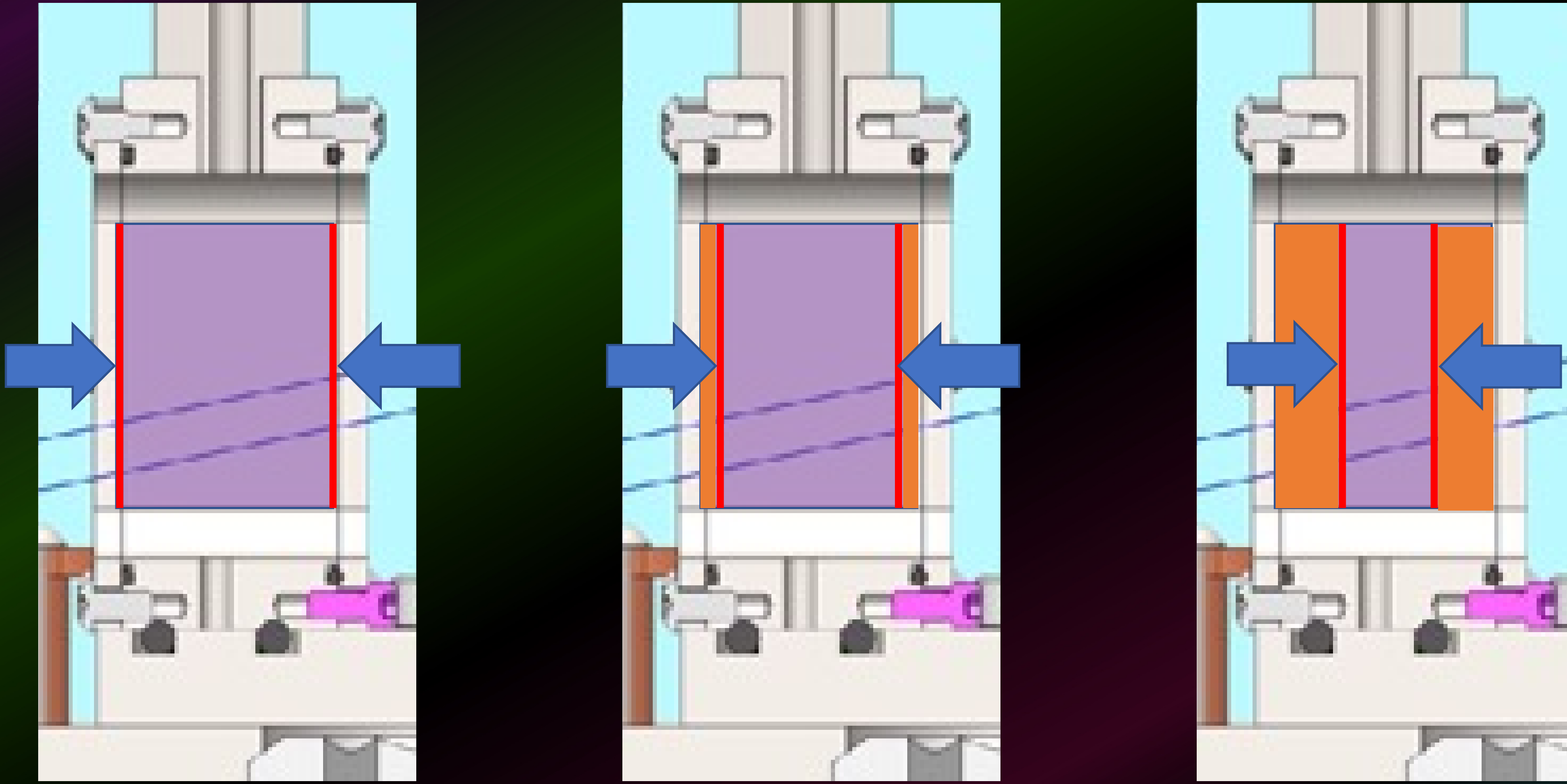

Simulations predict a central region of quasi hydro-unperturbed photoionized neon plasma

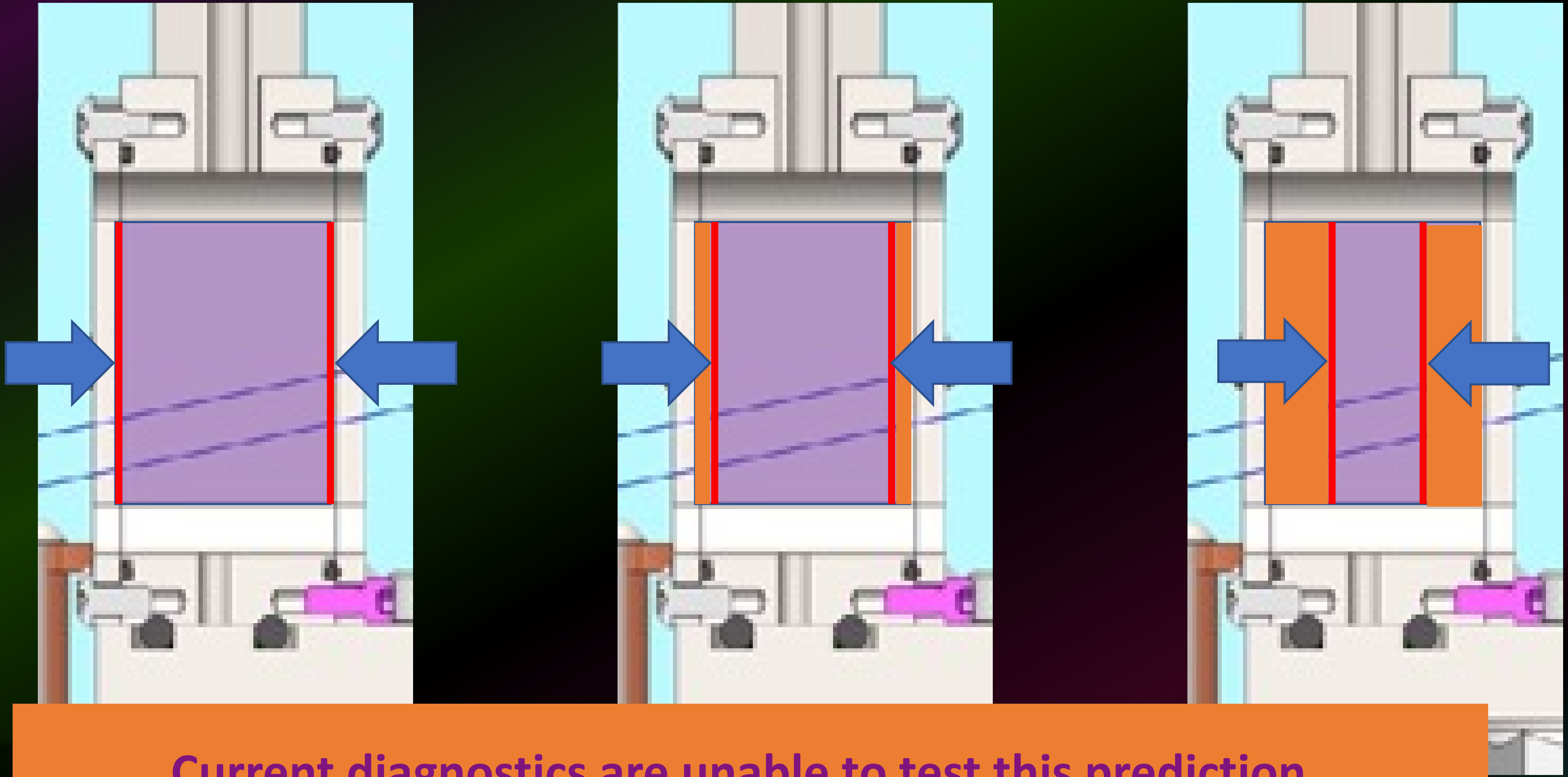

Current diagnostics are unable to test this prediction

Photon Doppler velocimetry enables measurement of electron density inside the gas cell

- From the time rate of change in optical path length, the time rate of change in the refractive index of a plasma can be inferred.[1]

$$\frac{d}{dt}\Delta_{OPL}(t) = -\frac{d}{dt}\int_{x_0}^{x_f} n(x,t)dx$$

- The index of refraction of the plasma is dependent on the electron density.

$$n(n_e) = \sqrt{1 - \frac{n_e}{N_c}} = \sqrt{1 - \frac{(e\lambda)^2 n_e}{m_e \varepsilon_0 (2\pi c)^2}}$$

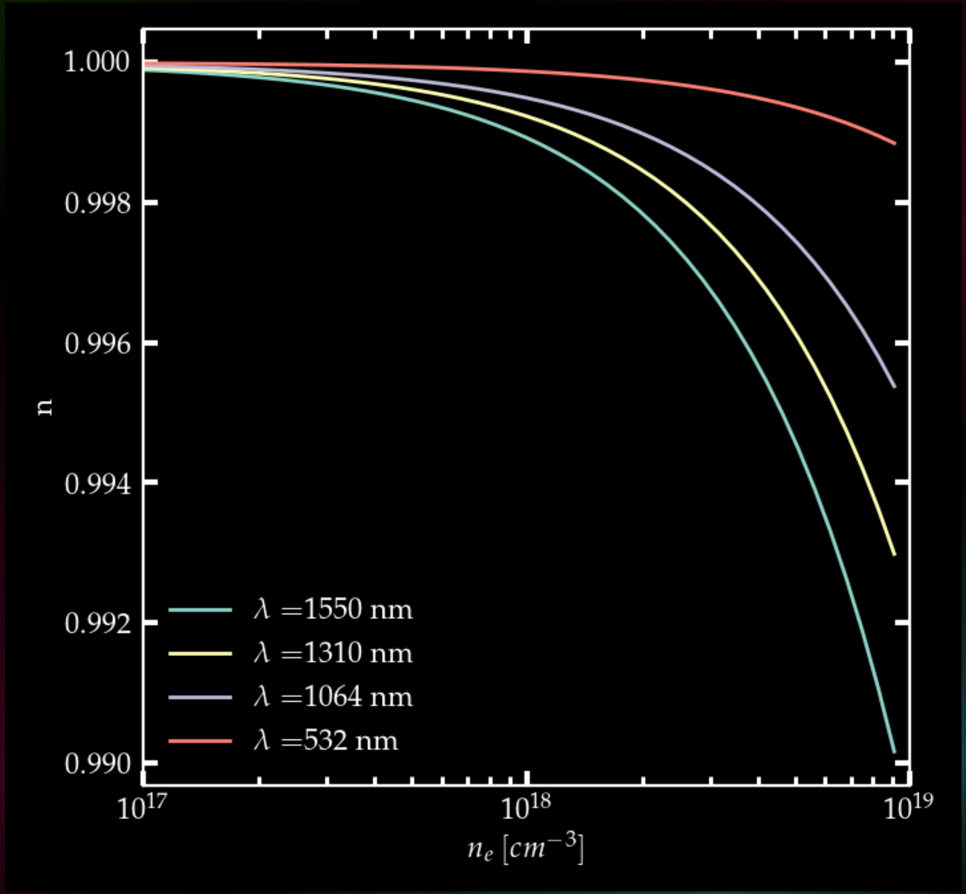

1) D. Dolan et al. JAP, 123, 034502, (2018)

Plasma uniformity can be assessed with two PDV probes

1. Assess the uniformity of the photoionized plasma in the gas cell via two PDV probes

2. Measure the electron density of the photoionized plasma within the gas cell

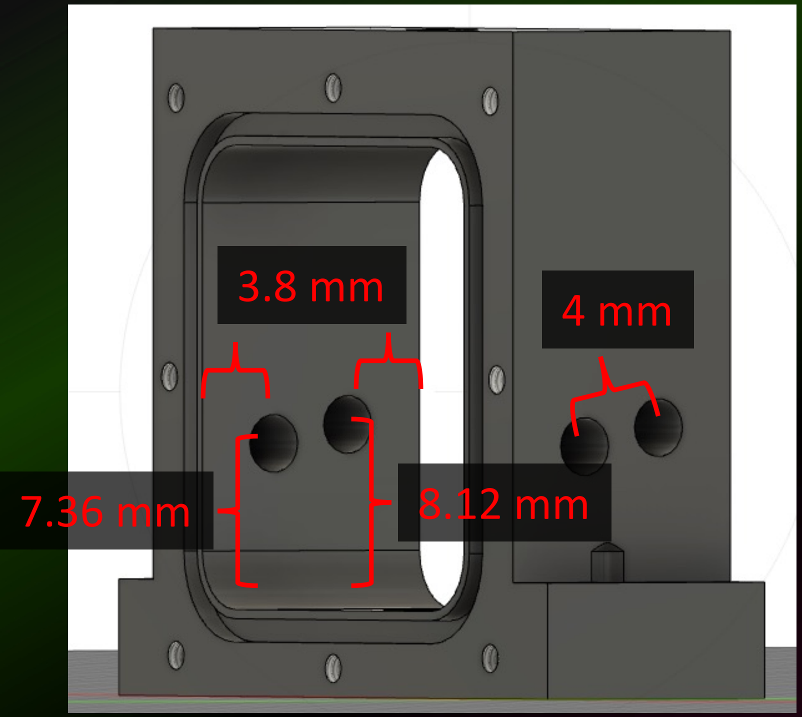

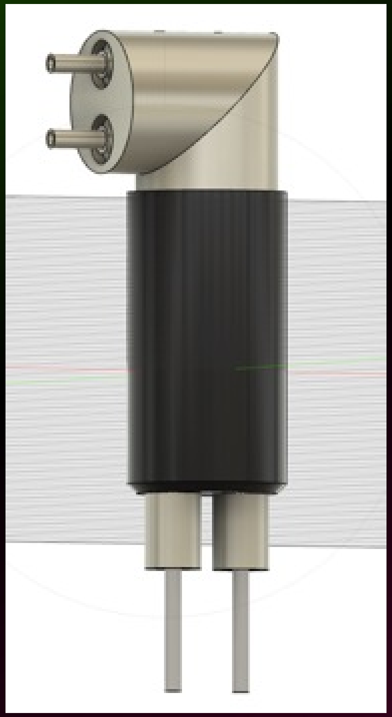

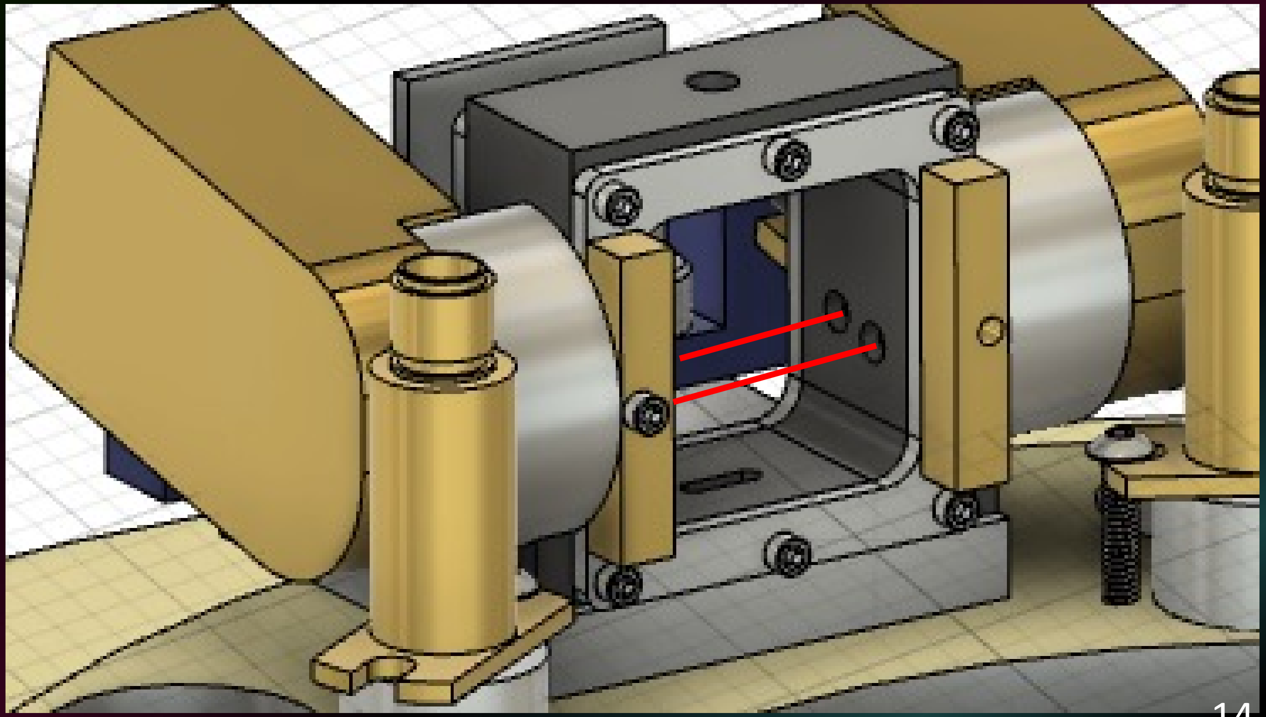

Fiber optic placement is a key consideration in extreme radiation environments

1. Fiber optics are susceptible to extreme radiation environments
    - 1-2 MJ of x-rays and ~ 200 TW of x-ray power
    - Gas cell placement ~ 6 cm from the z-pinch
    - Opposite effect of plasma detection with PDV

2. Gas cell footprint constrained by the anode B-dots
    - 90° dual fiber optic mirror assemblies were developed
        - Reduce exposed surface area of fibers
        - Avoid interference with anode hardware

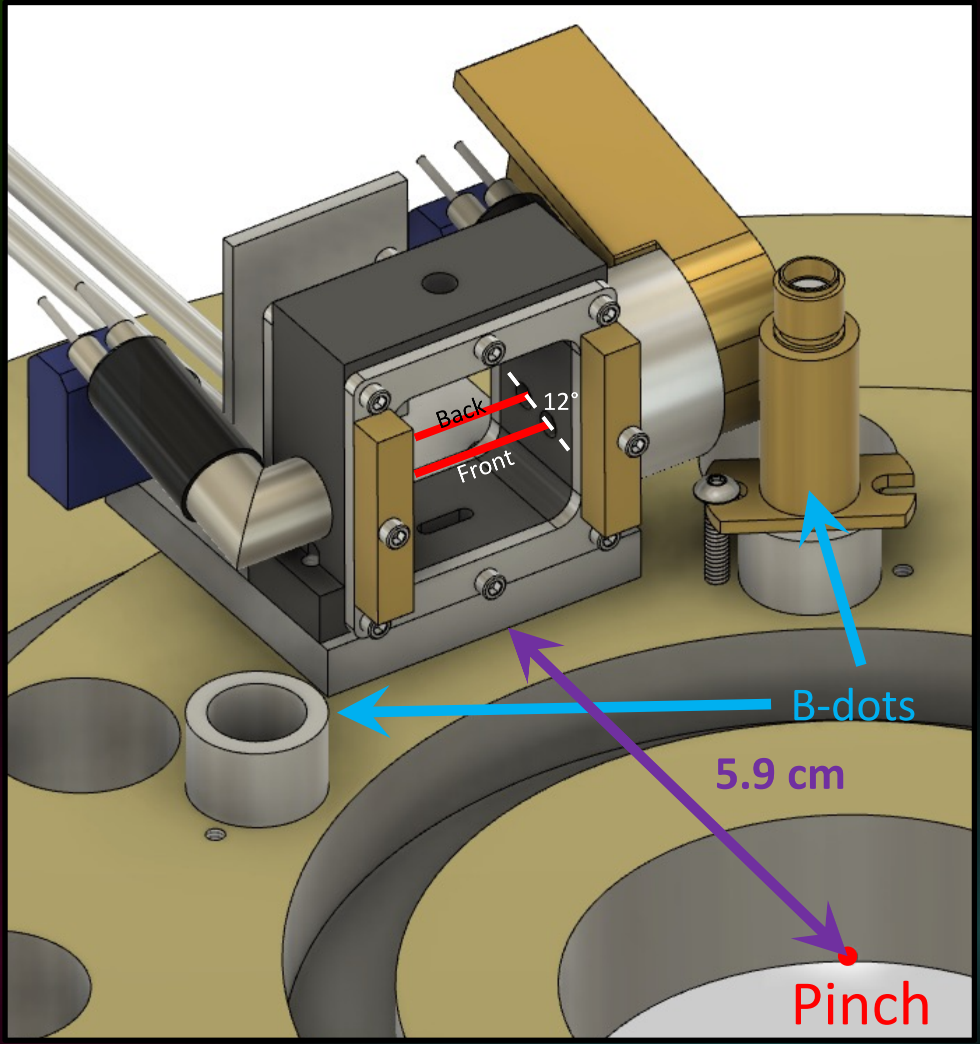

Challenge: Fiber optics are susceptible to extreme radiation environments

- Ionizing radiation can contaminate the fiber signal

- Radiation shielding is crucial for the implementation of PDV in close proximity to the pinch radiation

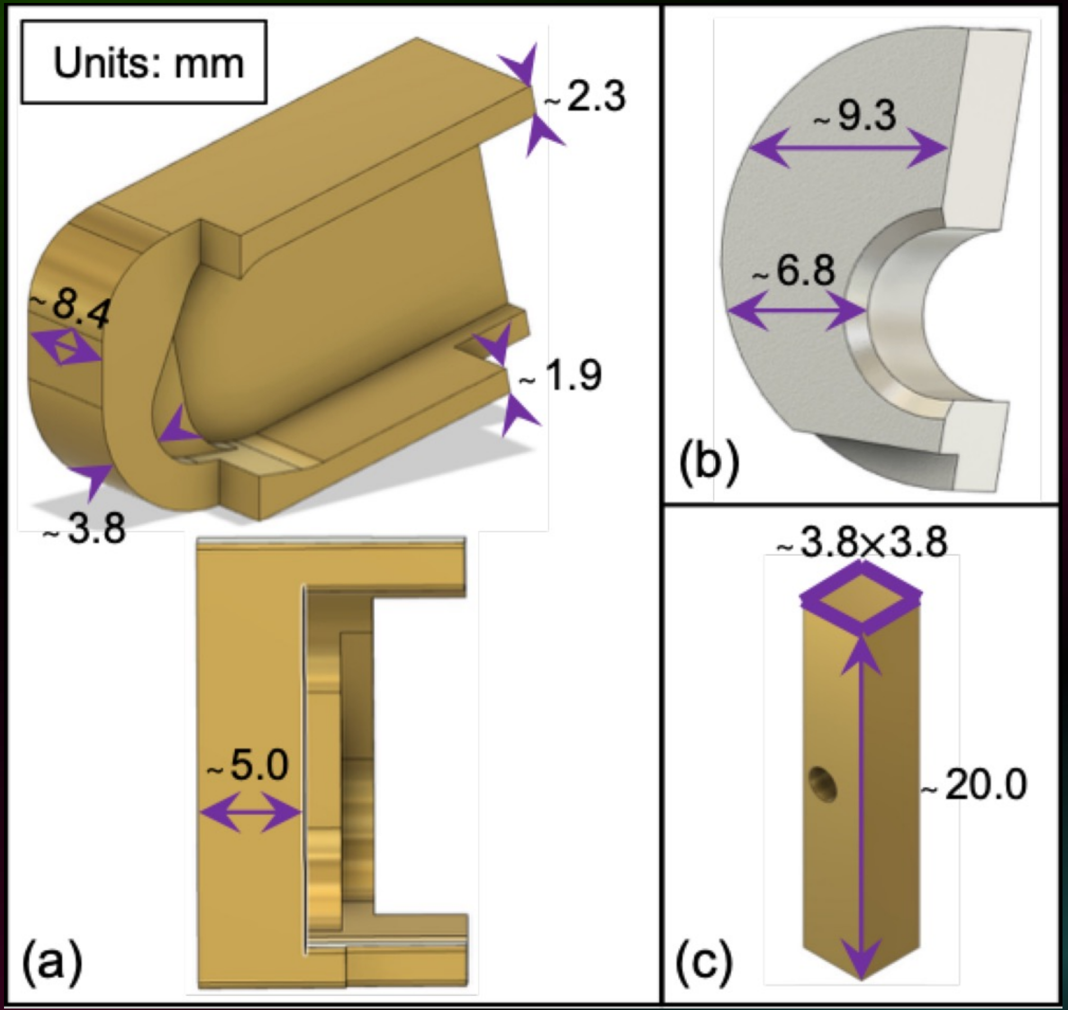

1. K. J. Swanson et al. RSI, 93.4, 043502, (2022)

Adverse radiation effects were crucial to mitigate and characterize

- Uni-directional PDV probes were located on both sides of the cell

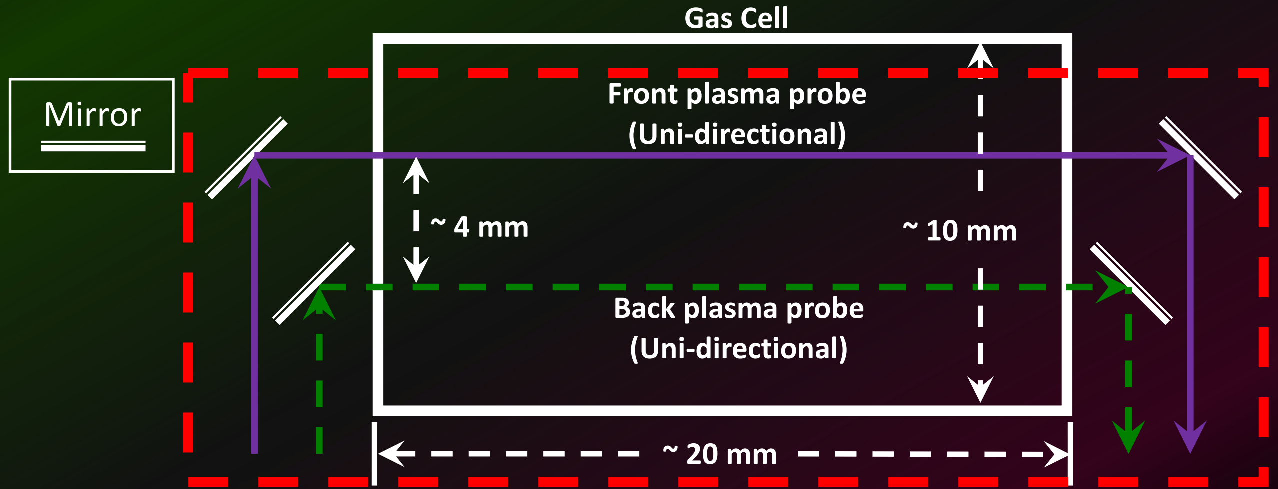

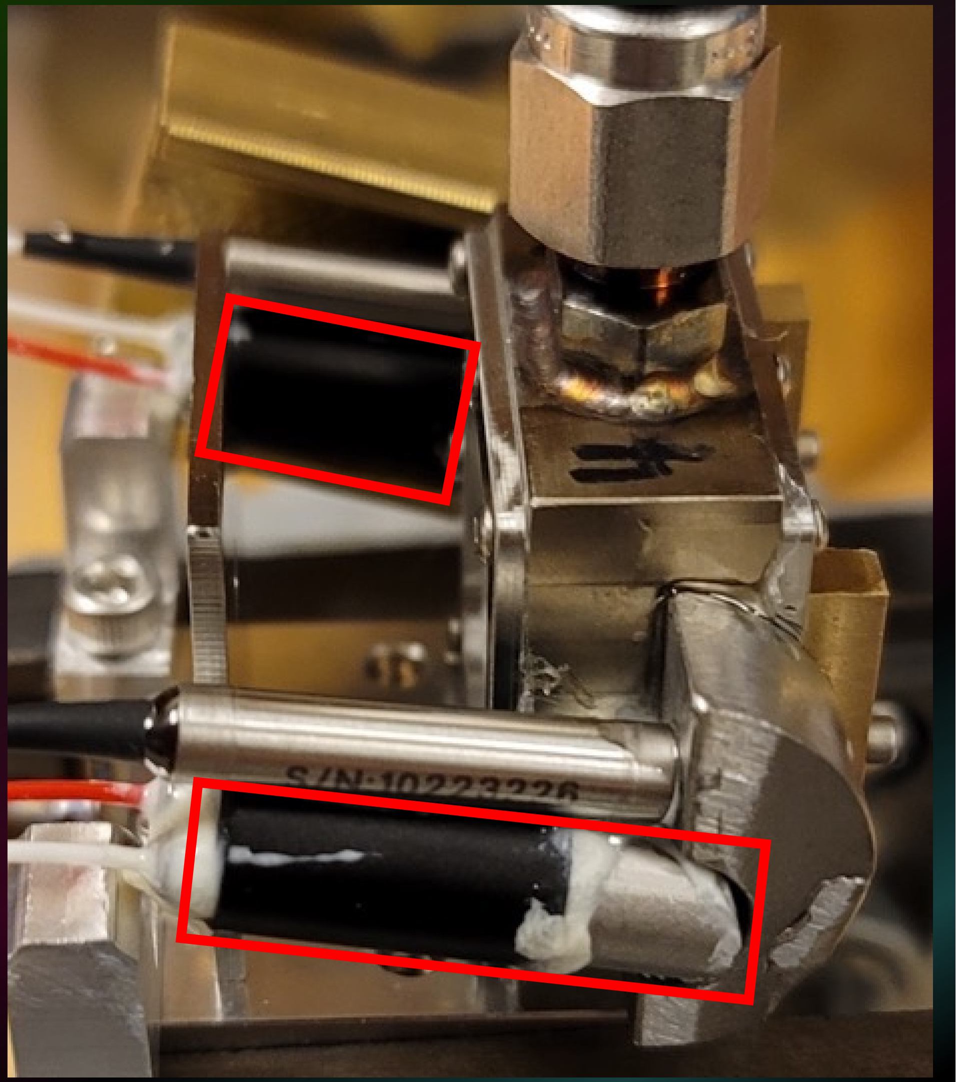

Radiation effects induced in the fiberoptics were characterized using PDV noise probes

- Bi-directional PDV probes with **mirrors** on the end were included on the right and left side of the gas cell

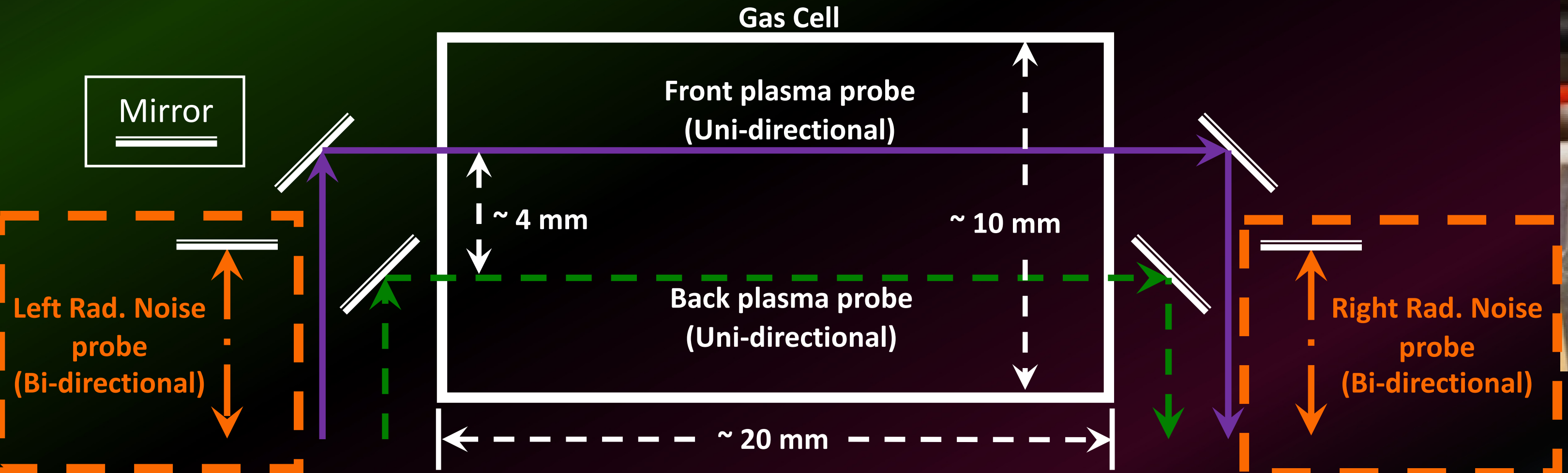

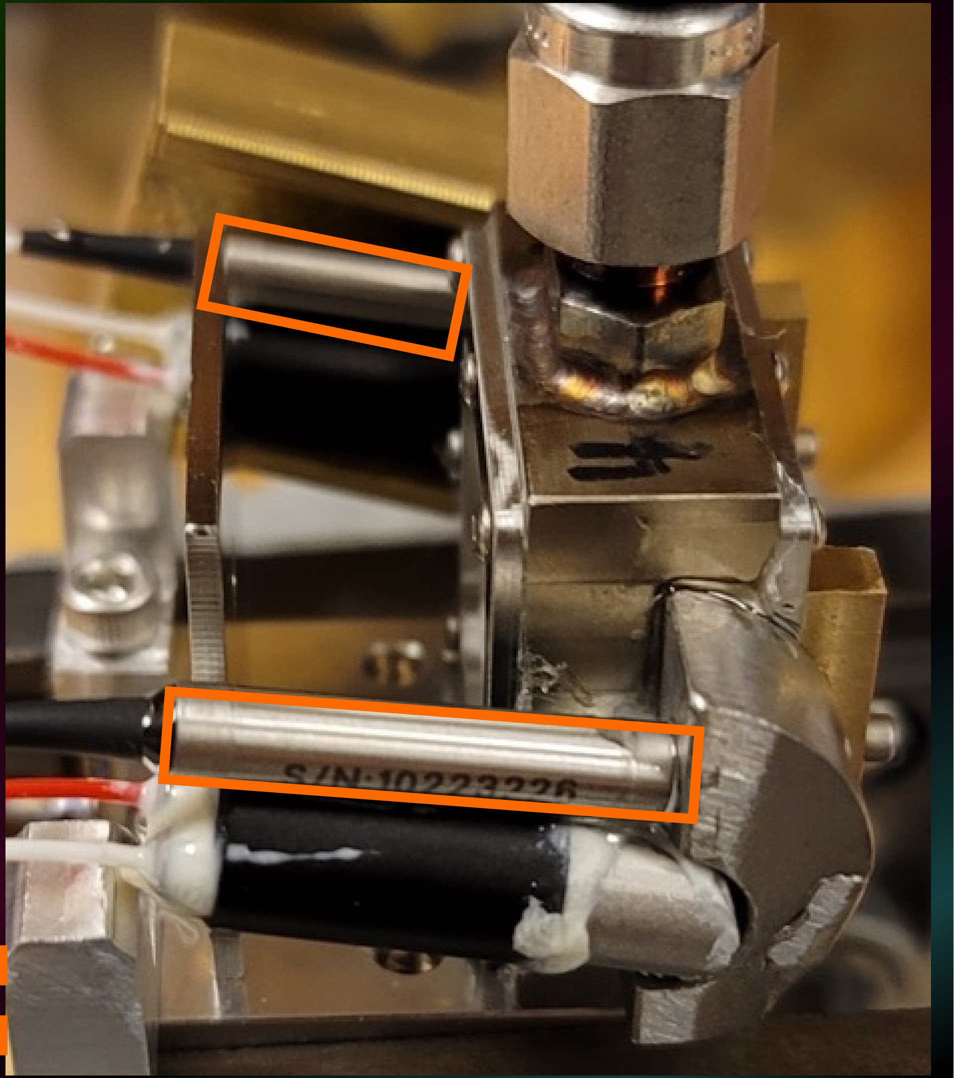

First direct observation of the early ionization radiation phase

- Early Ionization Phase
  - Lasts ~50 ns prior to the main x-ray pulse
  - Lower energy radiation
  - Driven by radiation from z-pinch produced by the run-in phase

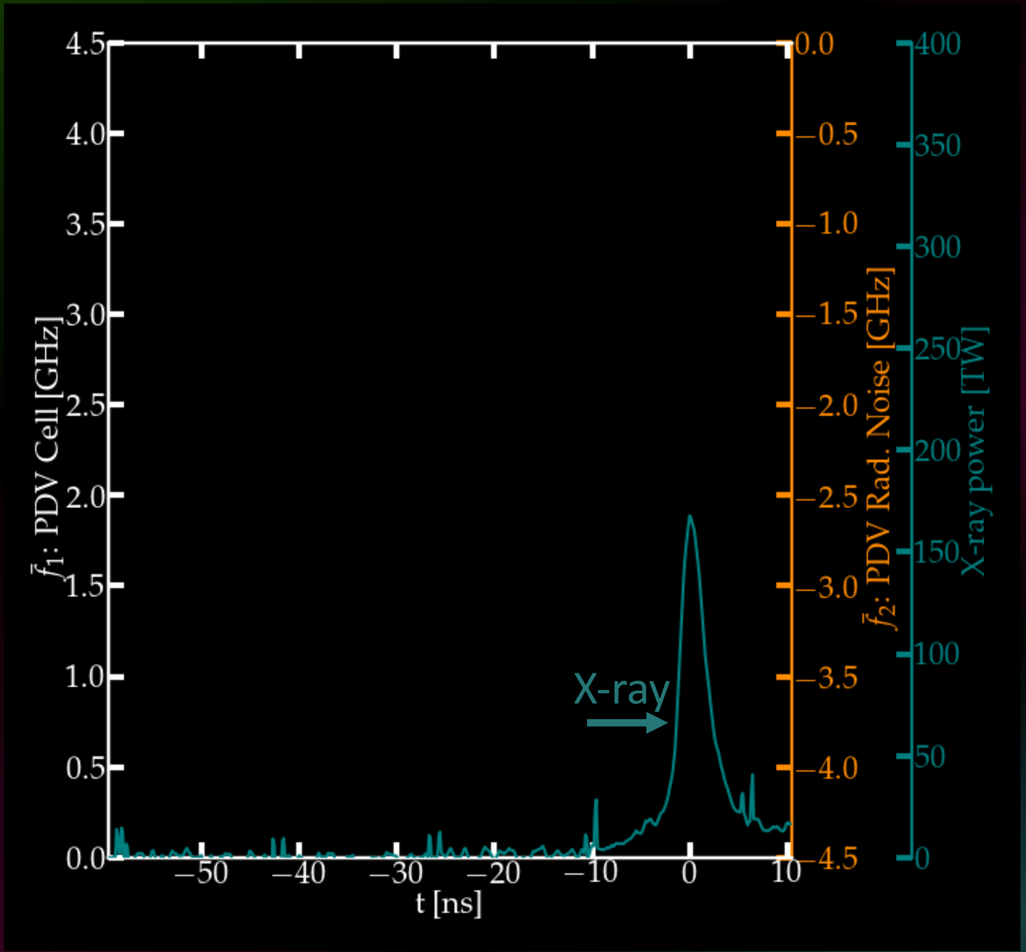

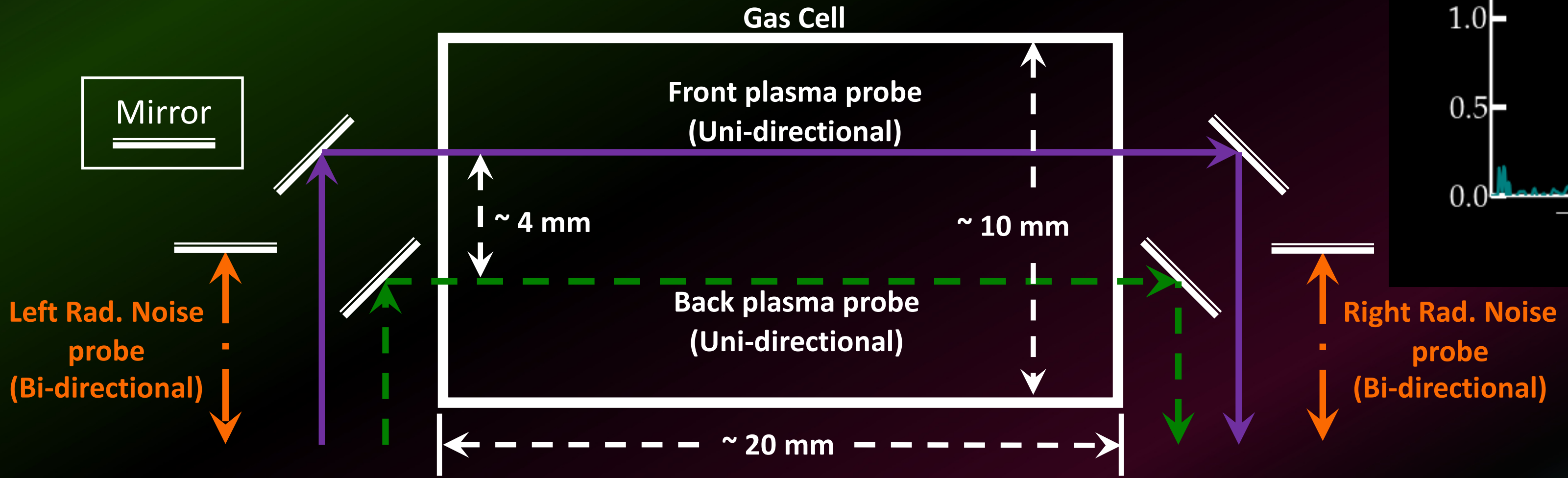

First direct observation of the early ionization radiation phase

- Early Ionization Phase
  - Lasts ~50 ns prior to the main x-ray pulse
  - Lower energy radiation
  - Driven by radiation from z-pinch produced by the run-in phase

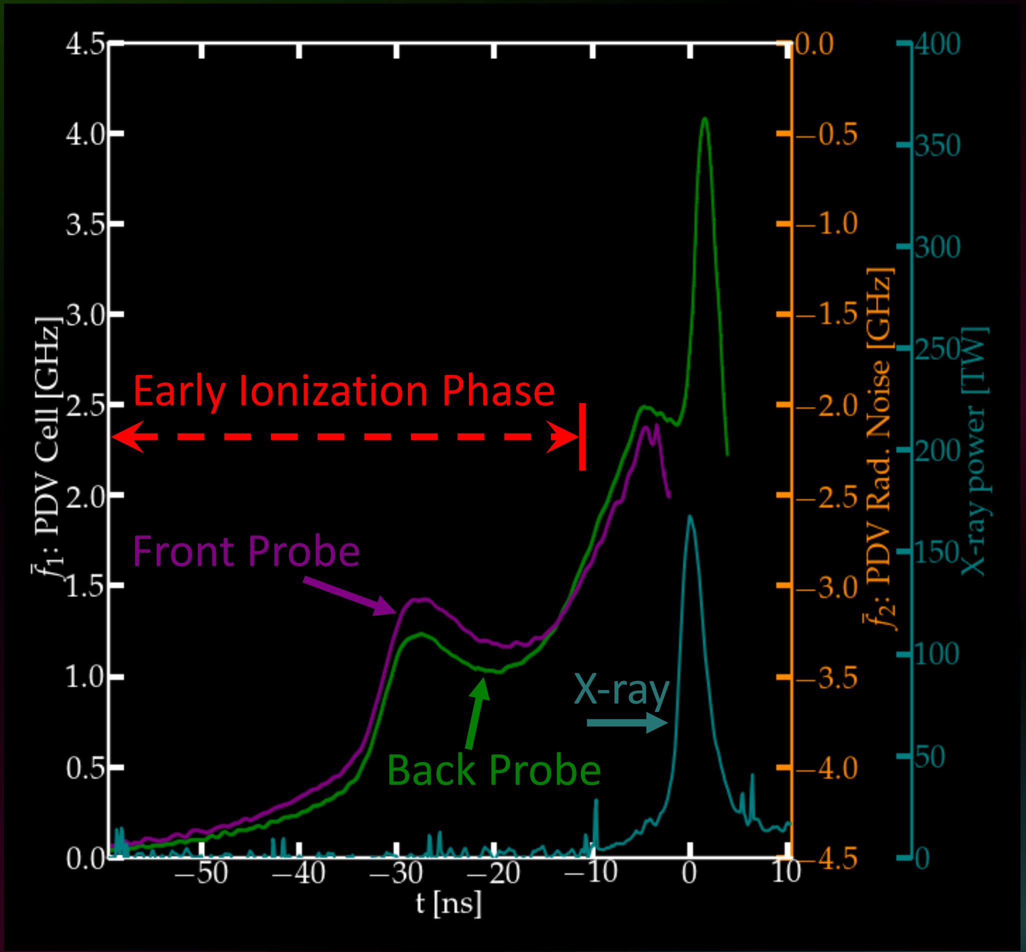

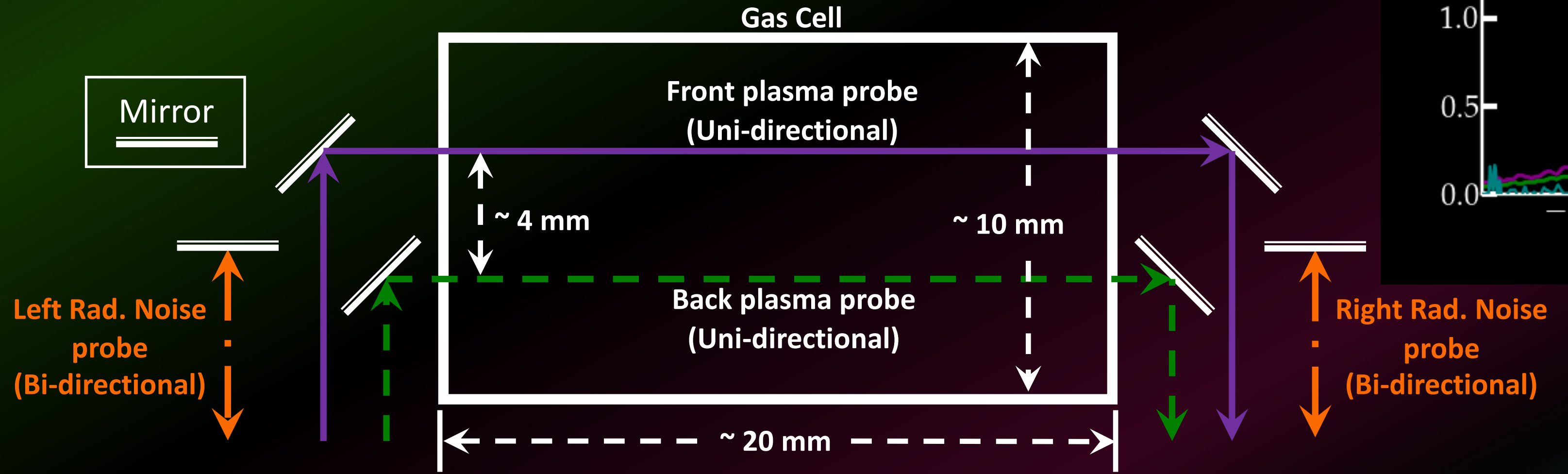

First direct observation of the early ionization radiation phase

- Early Ionization Phase
  - Lasts ~50 ns prior to the main x-ray pulse
  - Lower energy radiation
  - Driven by radiation from z-pinch produced by the run-in phase
- Radiation induced noise within the fiber optics is negligible

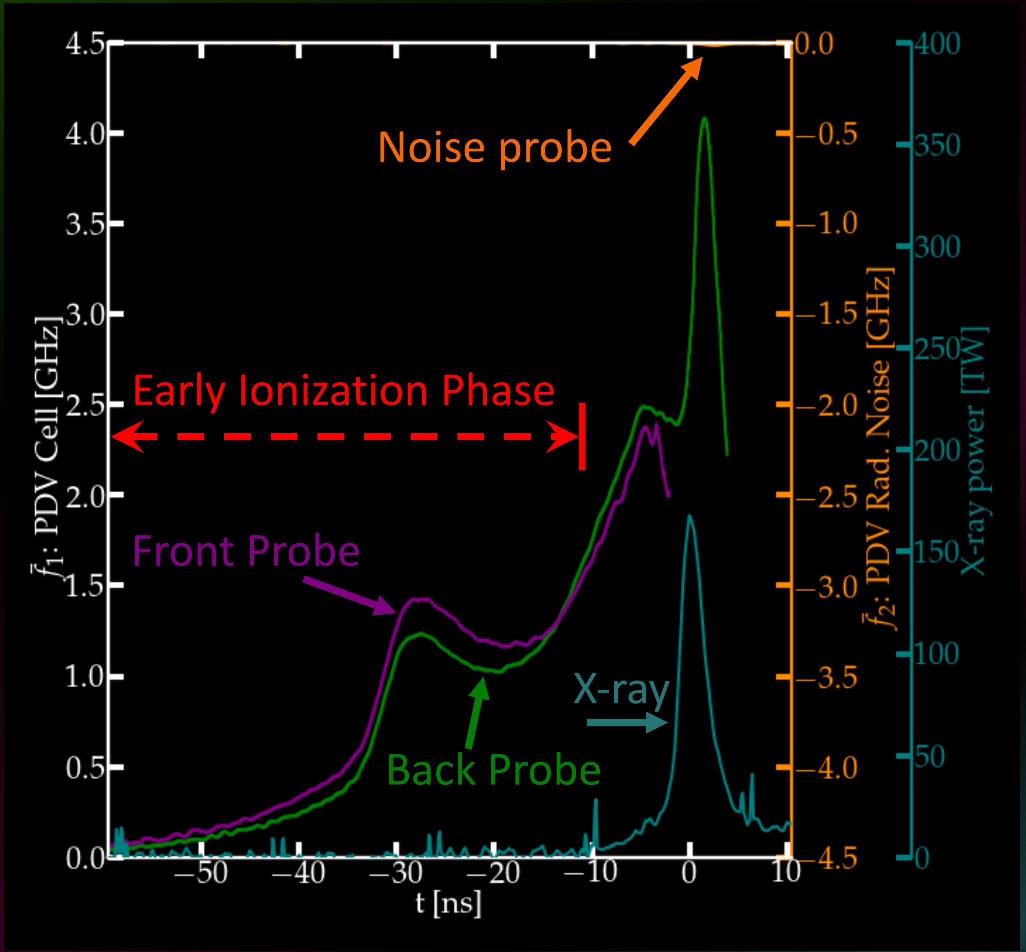

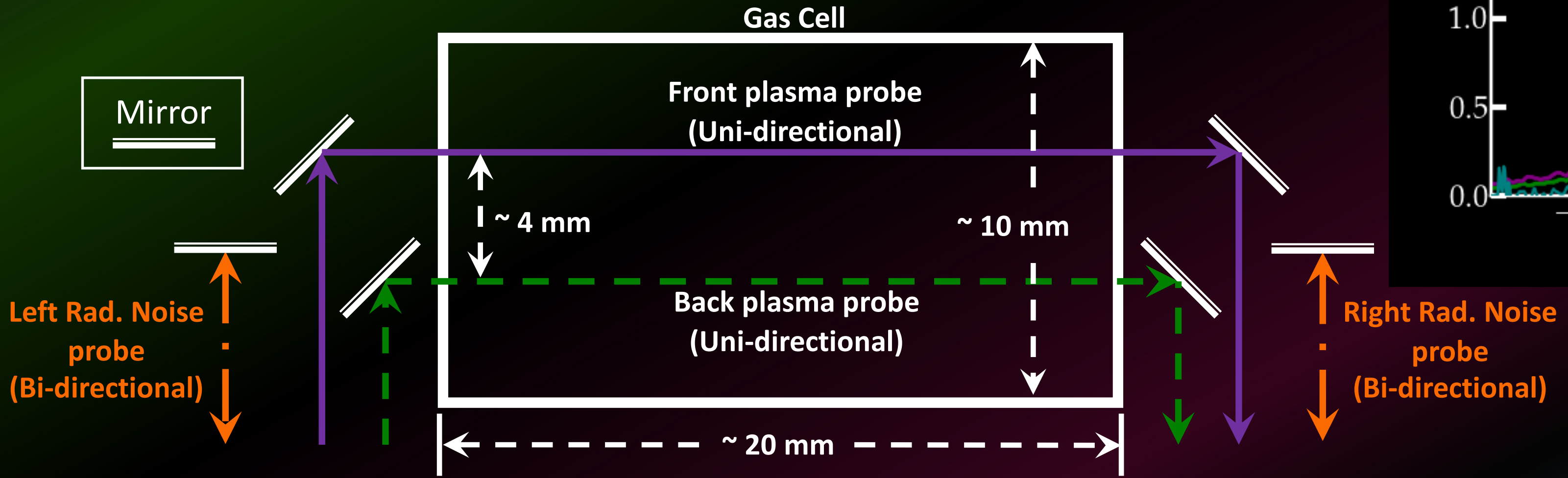

First direct observation of the early ionization radiation phase

- Early Ionization Phase
  - Lasts ~50 ns prior to the main x-ray pulse
  - Lower energy radiation
  - Driven by radiation from z-pinch produced by the run-in phase
- Radiation induced noise within the fiber optics is negligible

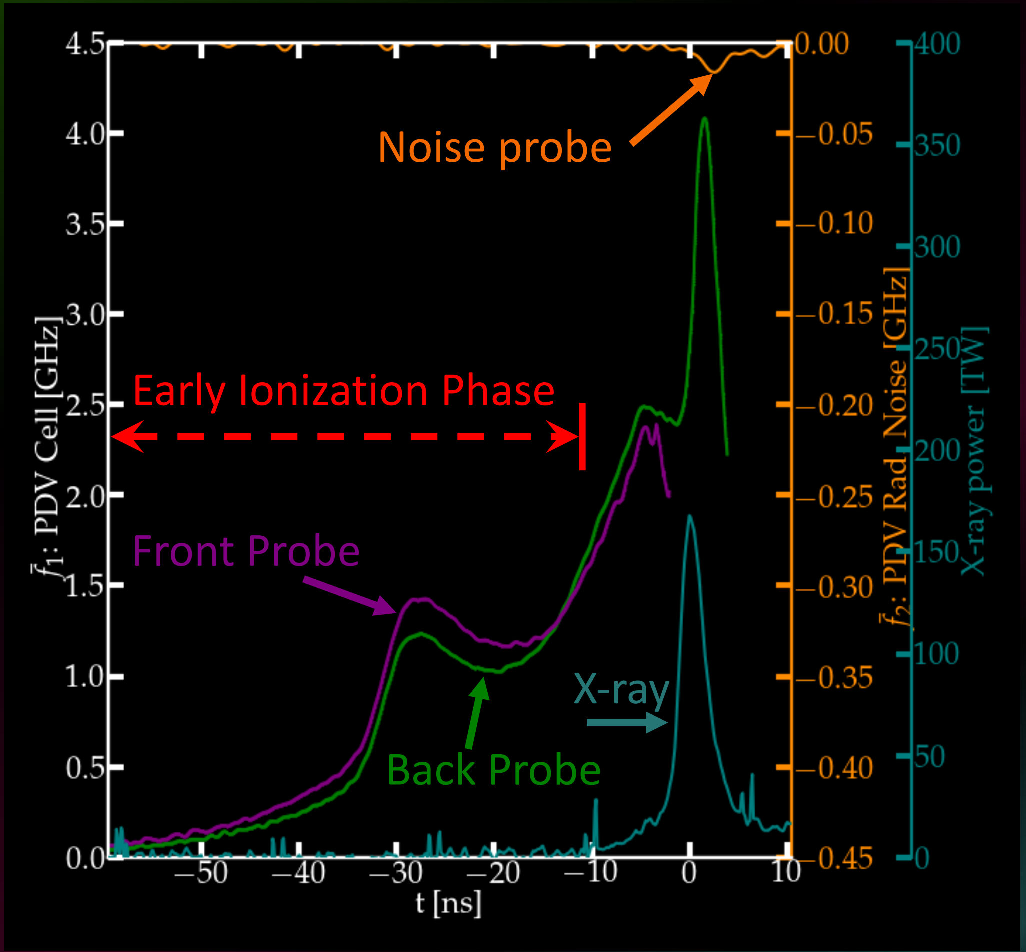

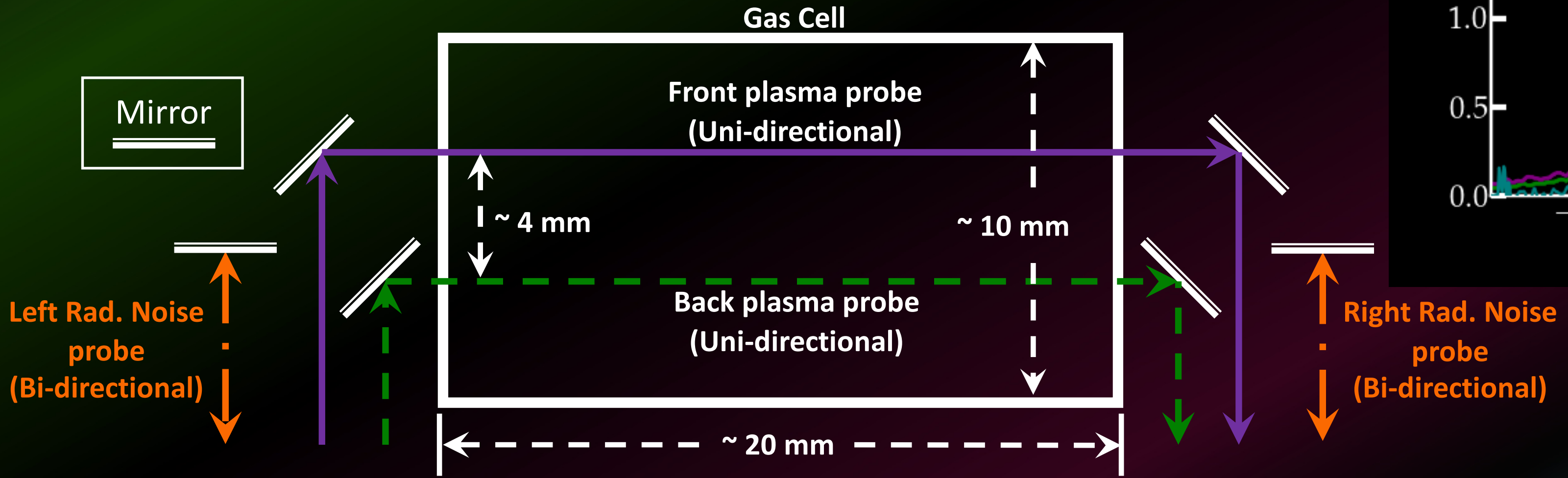

First direct observation of the early ionization radiation phase

- Early Ionization Phase
  - Lasts ~50 ns prior to the main x-ray pulse
  - Lower energy radiation
  - Driven by radiation from z-pinch produced by the run-in phase
- Radiation induced noise within the fiber optics is negligible
  - ~ 2 orders of magnitude lower

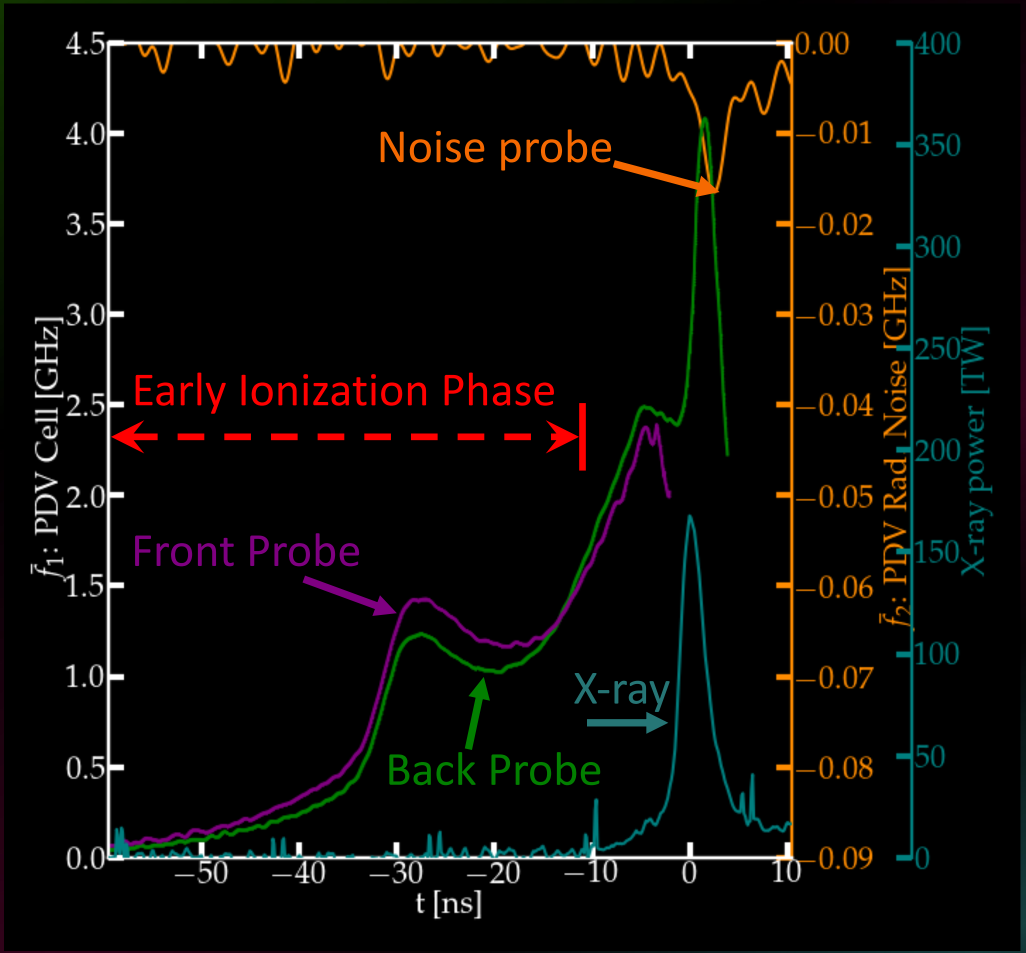

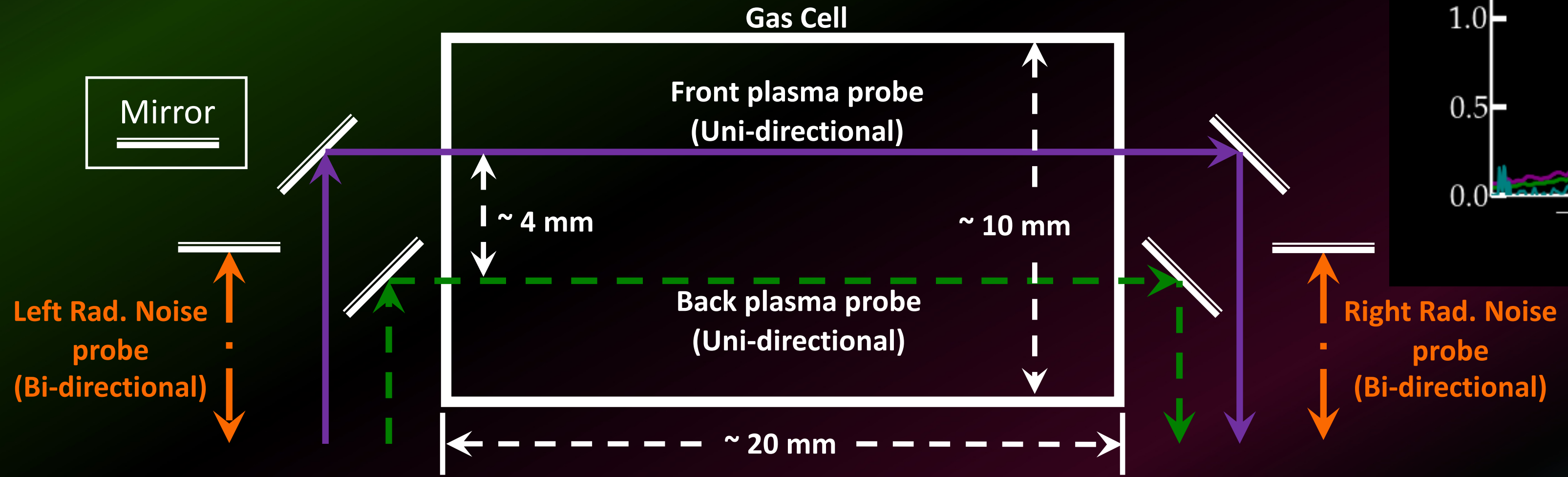

Differences in x-ray flux can be seen in the ionization rates between separate shots and between the front and back portion of the gas cell

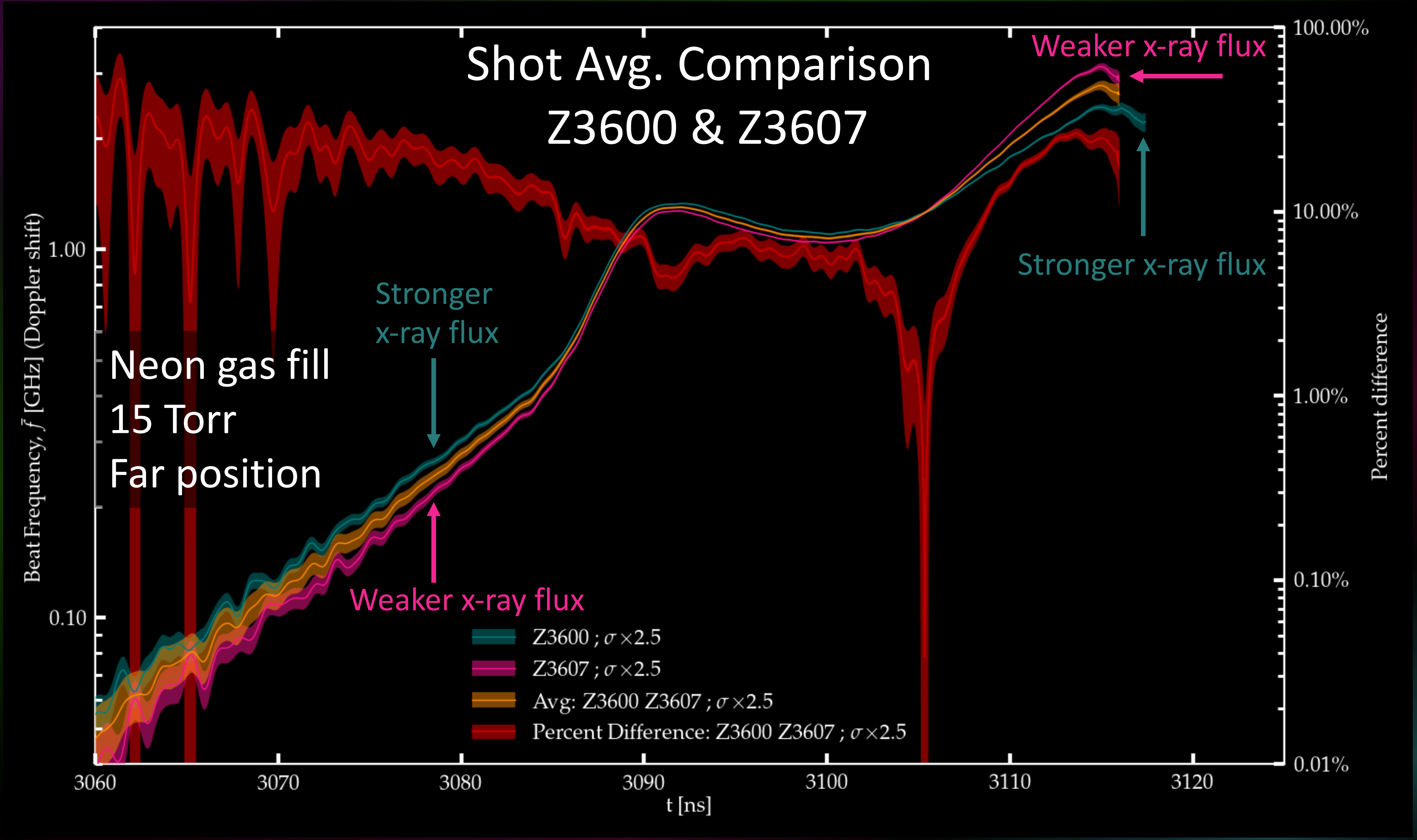

Differences in x-ray flux can be seen in the ionization rates between separate shots and between the front and back portion of the gas cell

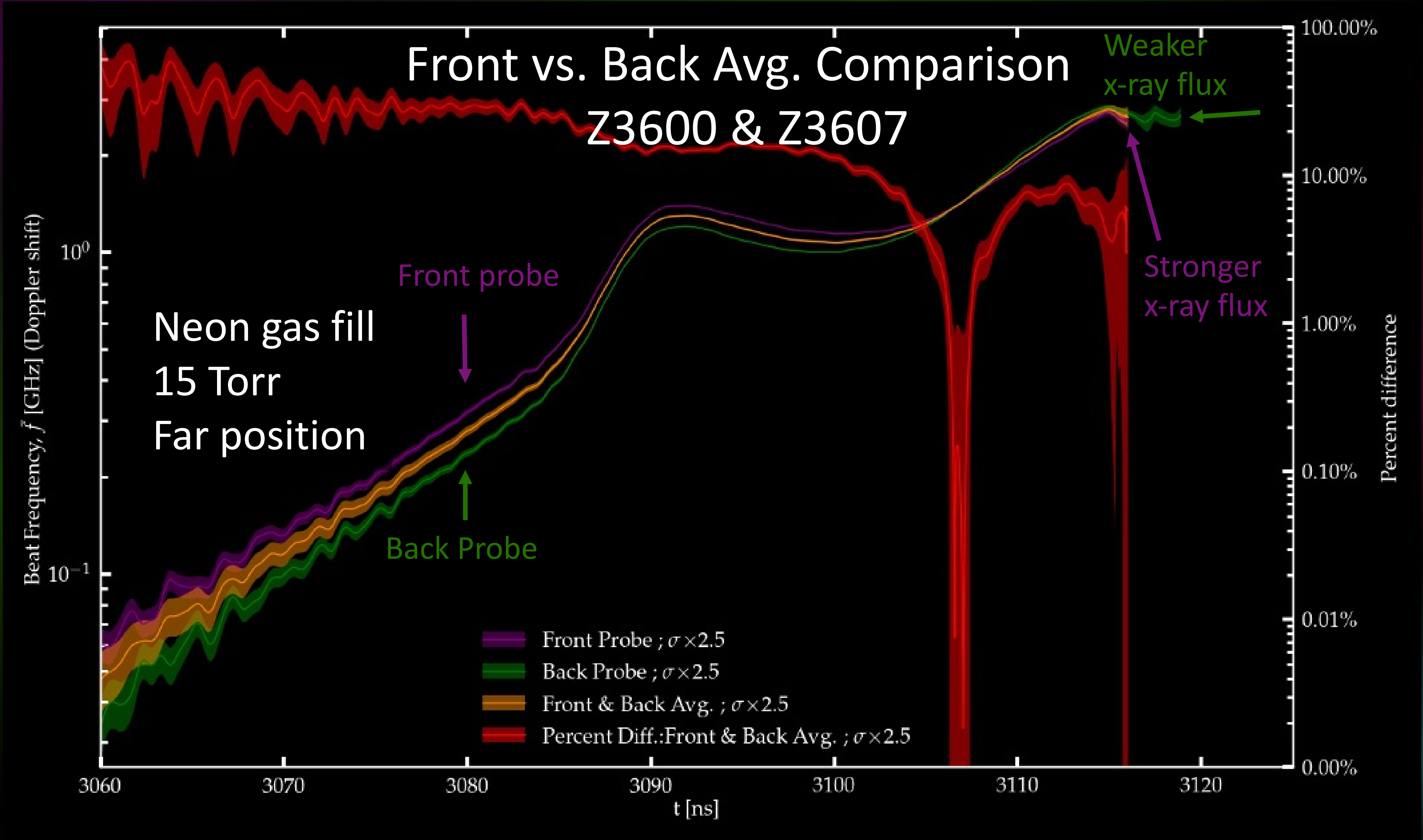

Comparison of radiation hydrodynamic simulations driven with two different levels of x-ray flux compare well with experiment

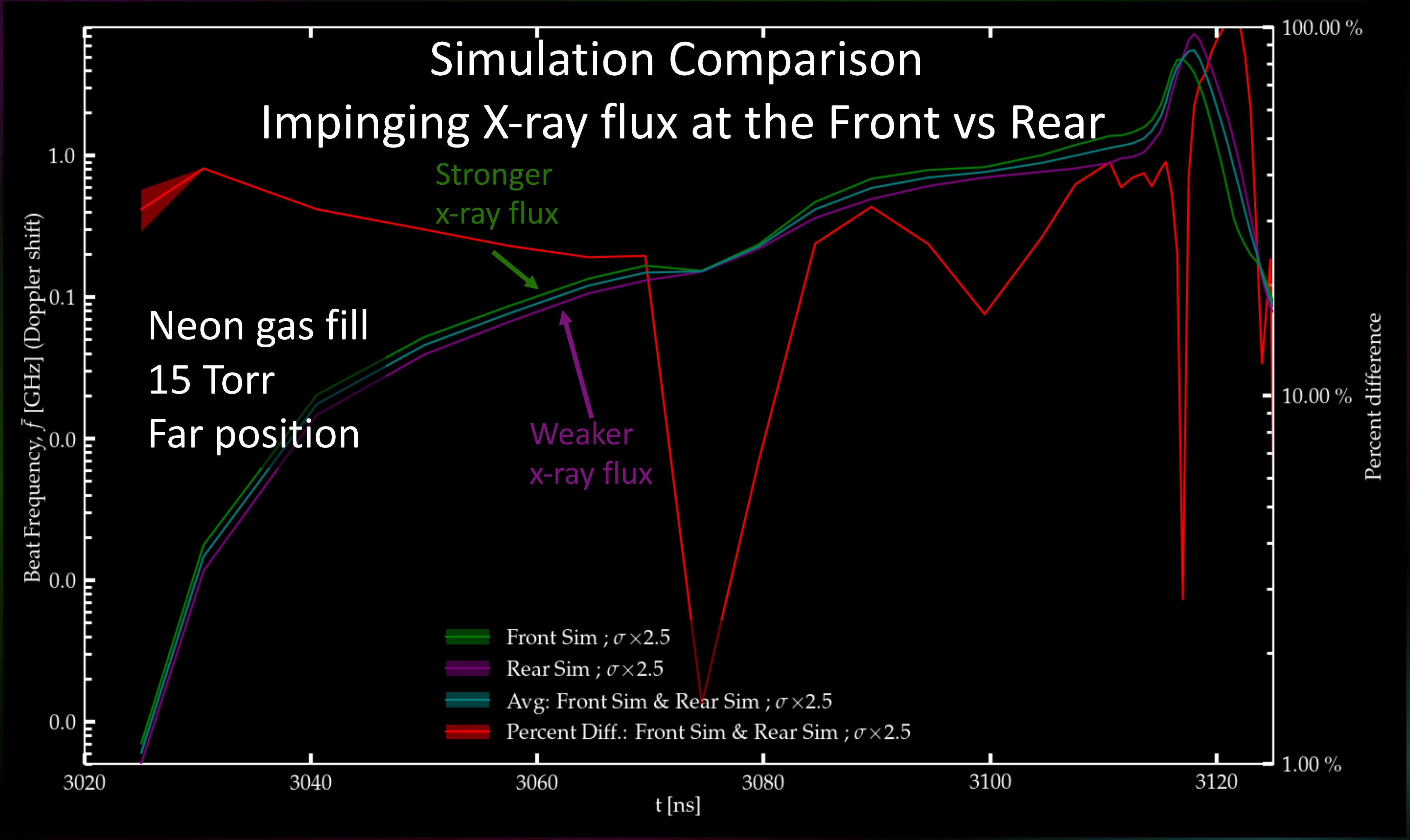

Comparison of radiation hydrodynamic simulations driven with two different levels of x-ray flux compare well with experiment

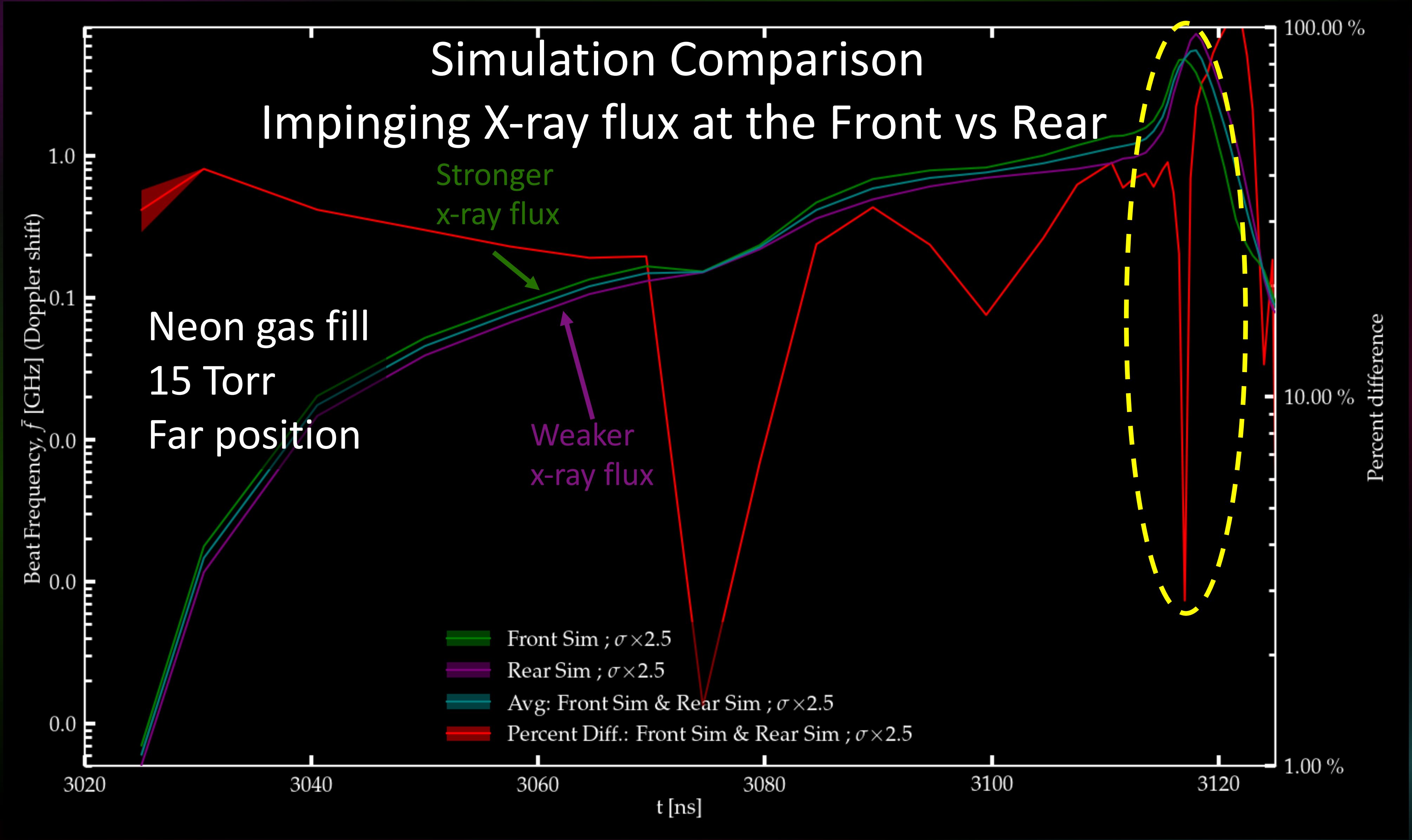

Comparison of radiation hydrodynamic simulations driven with two different levels of x-ray flux compare well with experiment

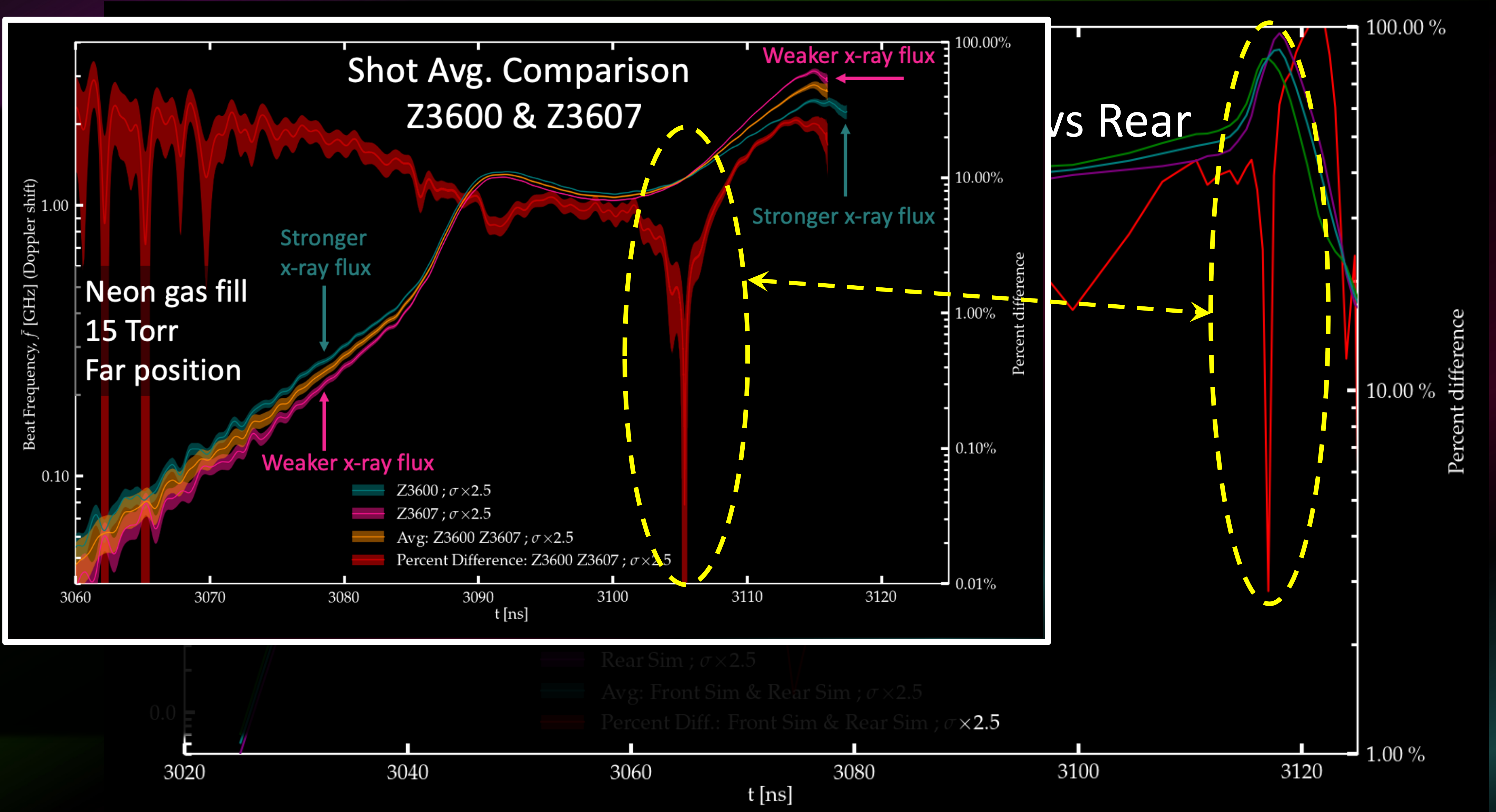

Comparison of radiation hydrodynamic simulations driven with two different levels of x-ray flux compare well with experiment

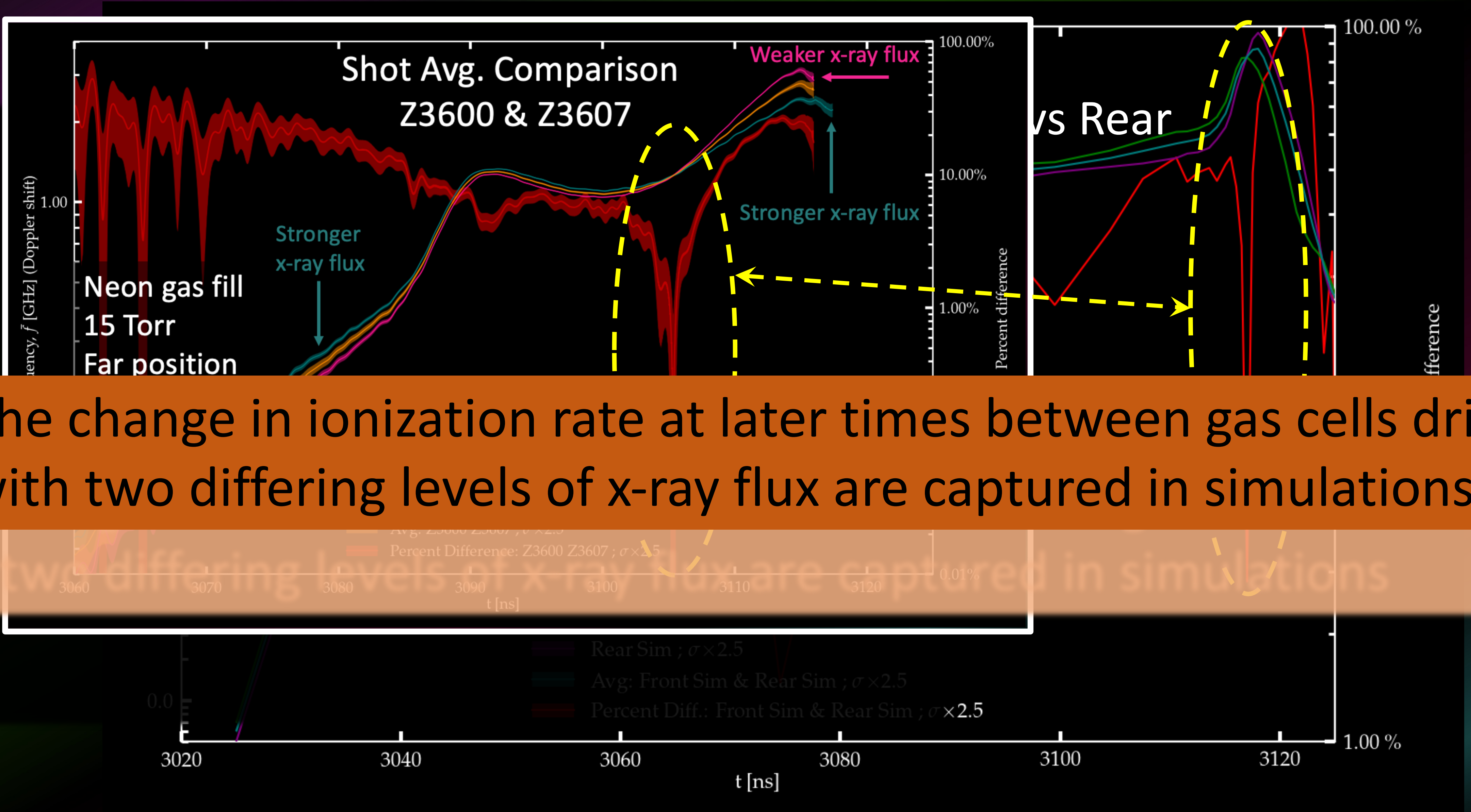

The change in ionization rate at later times between gas cells driven with two differing levels of x-ray flux are captured in simulations

Effect of early burst of radiation is captured by PDV diagnostic

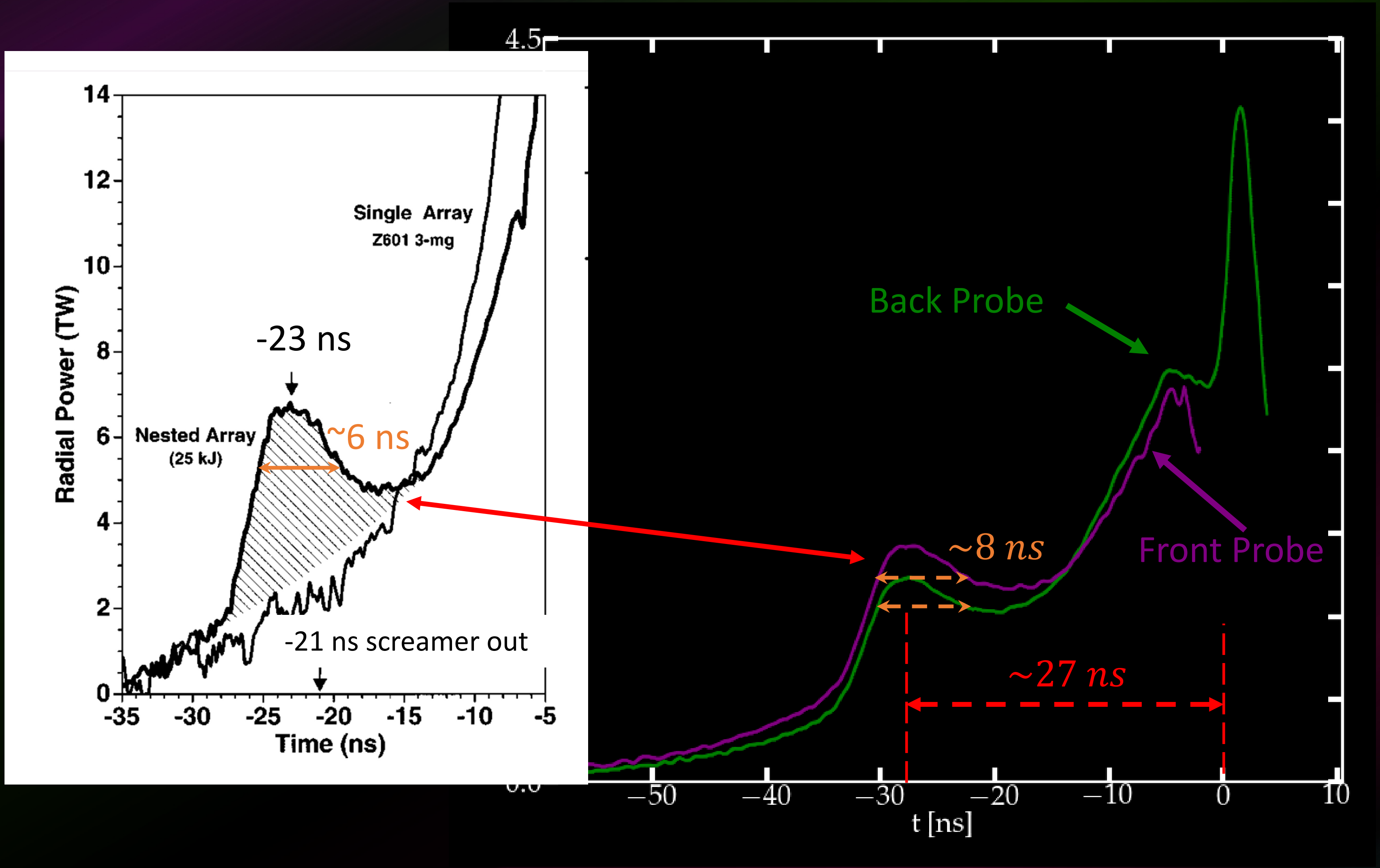

- First strike x-ray peak
  -23 ns
- Preheat ionization rate peak
  -27 ns
- First strike x-ray pulse width
  ~6 ns
- Preheat ionization pulse width
  ~8 ns

1. Sanford et al. POP, 9, 3573 (2002)

Time resolved electron density measurements are made possible with chordal interferometry

- Front probe observes rise in electron density before the back probe

- Nominally identical experiments show reasonable agreement
  - Neon @ 15 Torr: Z3600 & Z3607

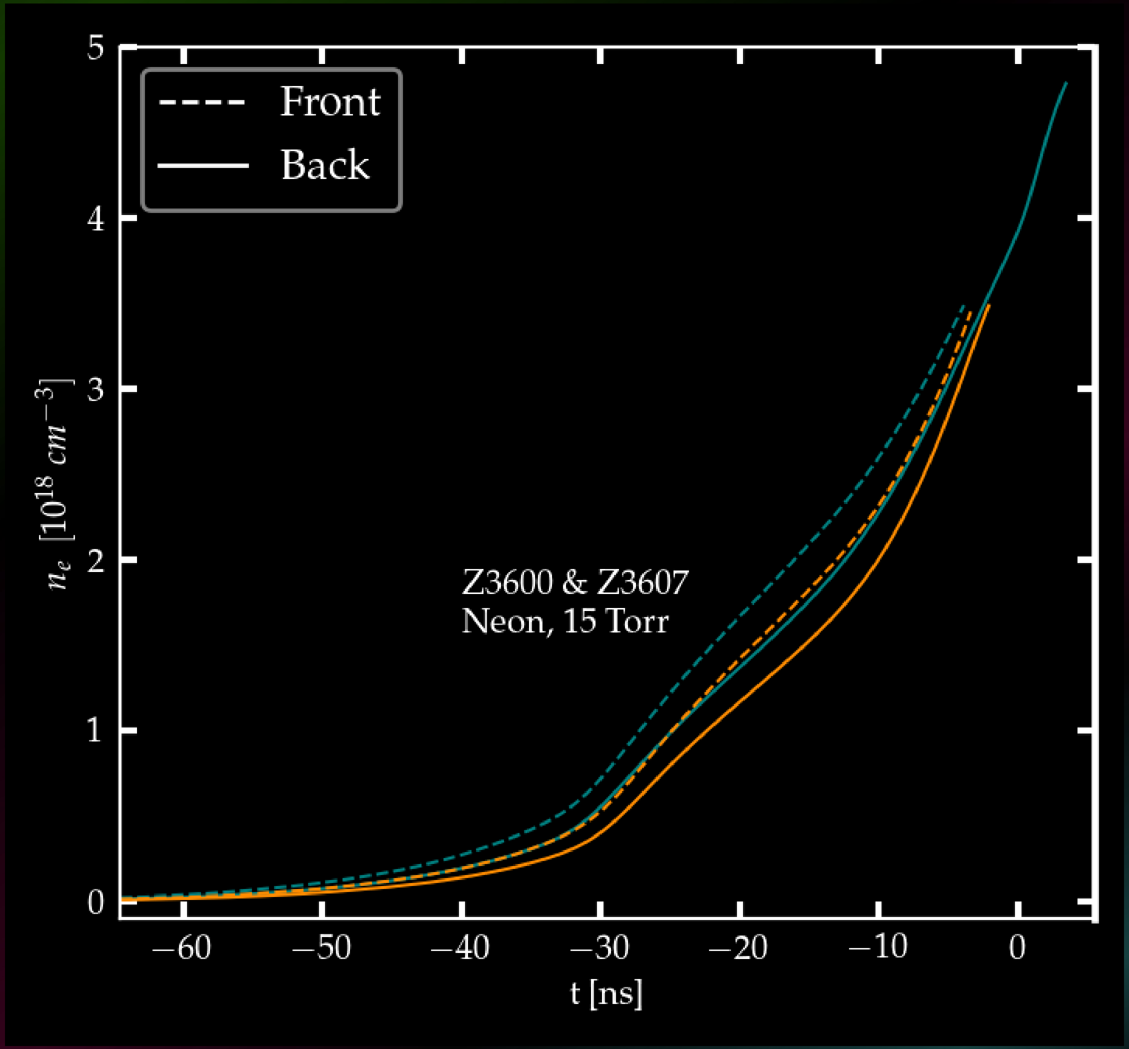

Time resolved electron density measurements are made possible with chordal interferometry

- Front probe observes rise in electron density before the back probe

- Nominally identical experiments show reasonable agreement
  - Neon @ 15 Torr: Z3600 & Z3607

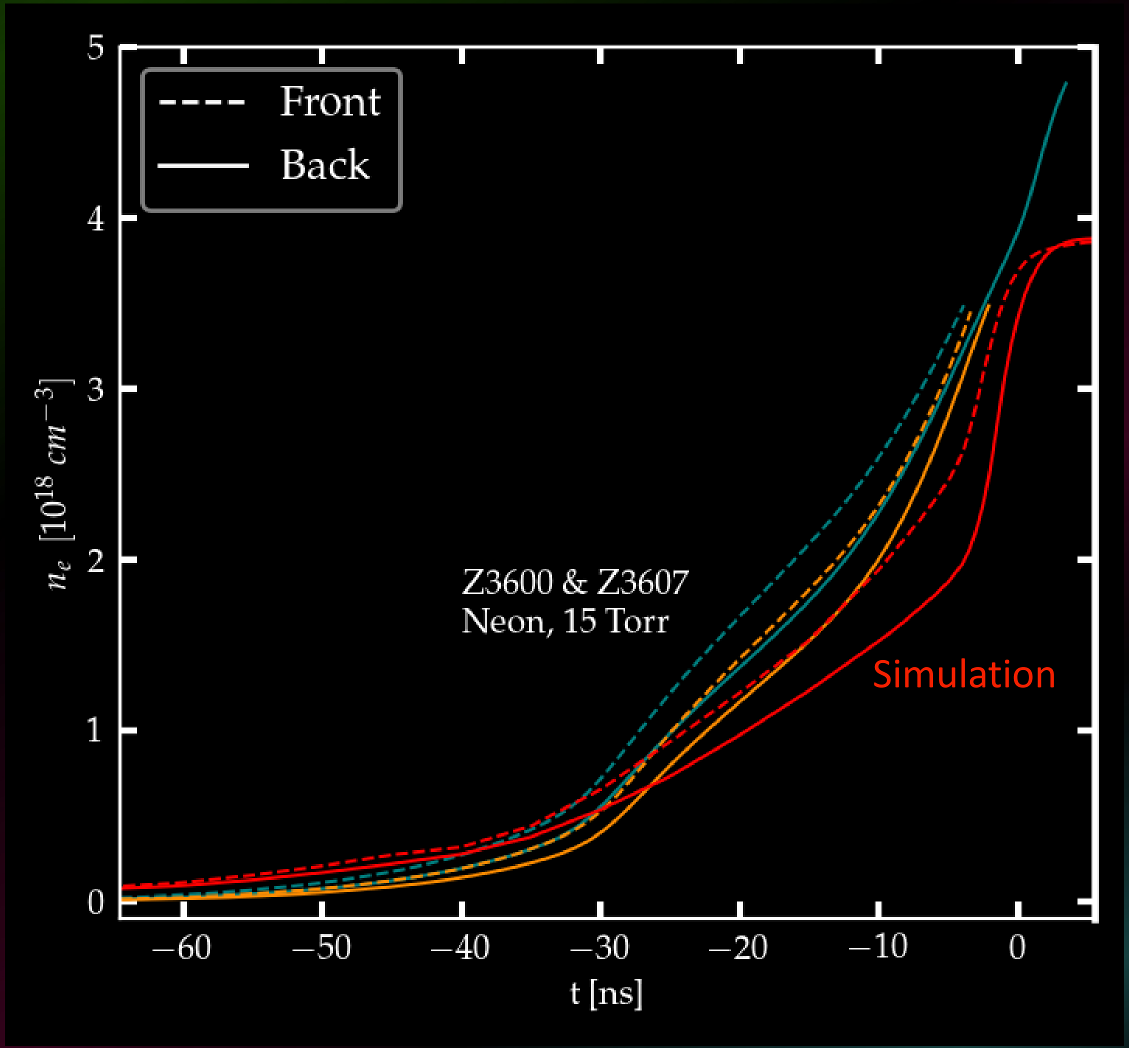

Time resolved electron density measurements are made possible with chordal interferometry

- Front probe observes rise in electron density before the back probe
- Nominally identical experiments show reasonable agreement
  - Neon @ 15 Torr: Z3600 & Z3607

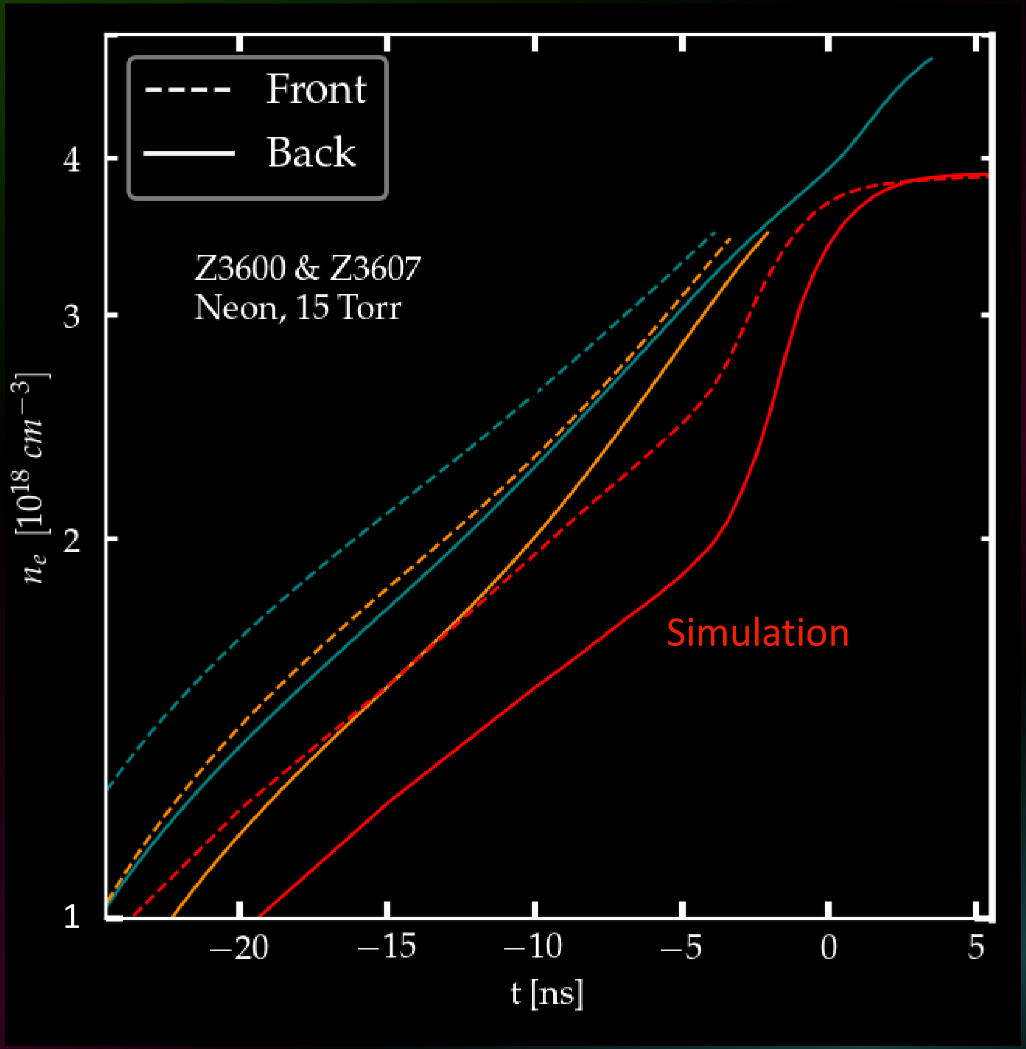

Time resolved electron density measurements are made possible with chordal interferometry

- Front probe observes rise in electron density before the back probe

- Nominally identical experiments show reasonable agreement
  - Neon @ 15 Torr: Z3600 & Z3607

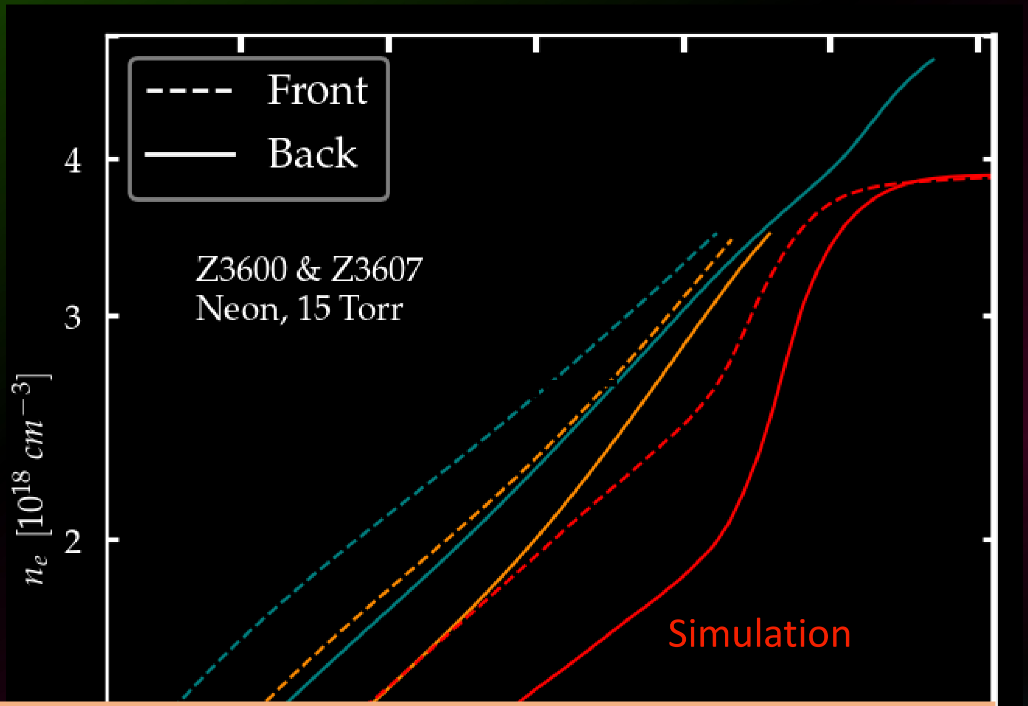

- **We can refine our understanding of experiments by combining laser and x-ray diagnostics**

- **As well we can test the accuracy of simulated electron density time histories**

A new interferometric diagnostic successfully revealed electron-density time histories of laboratory photoionized plasma for the first time

- Time and spatially resolved measurements of electron density time are a critical plasma diagnostic
- Photon Doppler velocimetry has been successfully implemented in close proximity to the x-ray flux produced by Z
- Dual PDV probes were used to assess plasma uniformity

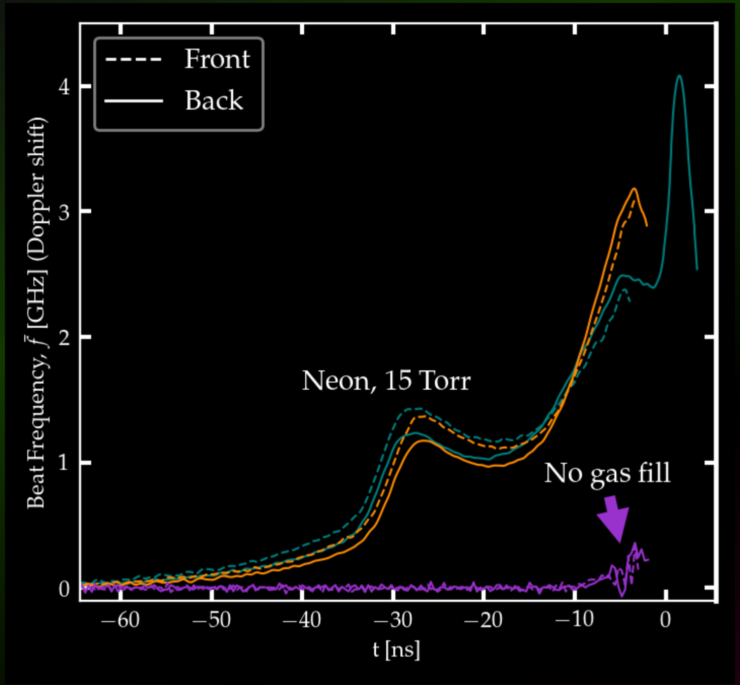

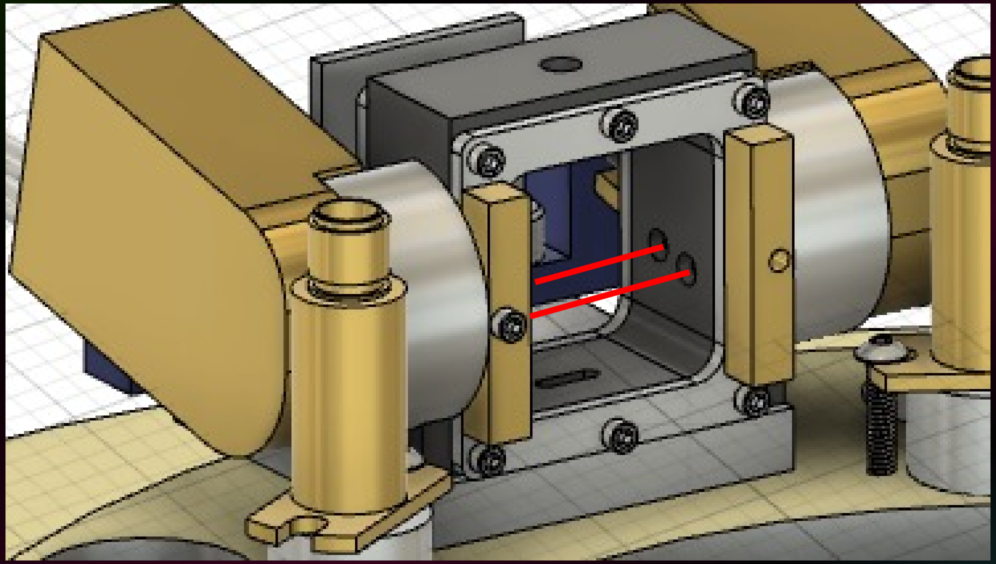

- We can refine our understanding of the experiment by combining laser and x-ray diagnostics
- We can test the accuracy of simulated electron density time history

This work was sponsored in part by DOE NNSA HEDLP Grant DE-NA0003875, the Wootton Center for Astrophysical Plasma Properties under U.S. Department of Energy cooperative agreement number DE-NA0003843, and the Z Facility Fundamental Science Program of Sandia National Laboratories. SNL is managed and operated by NTESS under DOE NNSA contract DE-NA0003525.